RESEARCH JOURNAL

AROR UNIVERSITY RESEARCH JOURNAL

Volume 02, Issue 02 (December-2025)

Annual Publication

Publisher: Aror University of Art, Architecture, Design & Heritage Sukkur

3106-9797

Patron-in-Chief Message

It is with immense admiration and admiration that I express my gratitude for the launch 2nd issue of the Aror University Research Journal (AURJ). As Patron-in-Chief, I believe this journal represents a significant milestone in our journey toward academic excellence, innovative research, and the preservation of our rich cultural heritage.

At Aror University, we are committed to fostering a vibrant culture of research and innovation that addresses contemporary global challenges while recognizing the unique traditions and values of our region. The AURJ is a vital platform for scholars, researchers, and practitioners from diverse fields, including art, design, heritage, and emerging technologies, to share groundbreaking ideas and transformative insights with a global audience.

In today's fast-paced world, interdisciplinary research and collaboration are essential for progress. The AURJ embodies this spirit by encouraging contributions that blend creativity with critical inquiry, ensuring that our research is not only advancing knowledge but also fostering significant social change.

I am particularly pleased to see this initiative align with our wider vision for Aror University, which emphasizes sustainability, inclusivity, and international collaboration. By publishing high-quality, peer-reviewed research, we aim to establish AURJ as a beacon of academic excellence and a catalyst for innovation across disciplines.

I express my gratitude to the editorial team, reviewers, and contributors for their dedication and dedication in making this journal a reality. I am confident that the AURJ will be a key component of scholarly engagement and will enhance Aror University's reputation as a center of academic distinction.

Let us continue to explore new frontiers of knowledge, inspire creativity, and contribute to the advancement of society.

Warm regards,

Prof. Dr. Zahid Hussain Khand
Vice Chancellor
Aror University of Art, Architecture, Design, and Heritage
Patron-in-Chief, AURJ

Editor-in-Chief Message

Dear Colleague,

It gives me great pleasure to introduce the 2nd issue of Aror University Research Journal (AURJ). AURJ is the inaugural peer-reviewed research publication of Aror University of Art, Architecture, Design and Heritage, located in the heart of the historic Indus Valley, one of the greatest and most ancient centers of culture and civilization in the world.

For more than five thousand years, the Indus Valley and the Sindh region have been both a center of civilizational development and a trading crossroads for diverse cultures, all of which have contributed to the magnificent heritage of the people of Sindh. As inheritors of this millenia-old heritage, our institutional mission at Aror University is focused on reviving traditional values and promoting the cultural and religious diversity of the Sindh region. Accordingly, AURJ has an especial, though not exclusive, interest in research related to art, architecture, archaeology, history, agriculture, and other fields of central relevance to the Indus region and its culture.

More broadly, AURJ aims to serve as a platform to bring together researchers from all disciplines in art, architecture, design, heritage, engineering, technology, and social and natural sciences. AURJ also aspires to be an interdisciplinary forum for sharing problems, solutions, novel ideas, case studies, and technologies in support of the goals of sustainable development.

We welcome submissions and queries for AURJ from academicians, researchers, and practitioners worldwide. At AURJ we are committed to scholarly professionalism. All submissions will be evaluated according to our double-blind peer review process, and all authors will receive prompt notification of editorial decisions.

We are humbly grateful for the opportunity to launch and participate in this new scholarly enterprise, and we welcome both your leadership and your research.

Dr. Steven Bonta
Editor-in-Chief
Publisher, American Opinion Foundation, USA

Editorial Team

Patron-in-Chief

Editor-in-Chief

Editors

Managing Editor

Reviewer Acknowledgement

Dr Abdul Sallam Brohi
Northwest institute Eco-Environment and Resources, Chinese Academy for Science, China.
Email: abdulsalam@nieer.ac.cn

Dr. Sufi Ruhal
Department of Civil Engineering
Dawood University, Karachi
Email: ruhal.memon@duet.edu.pk

Dr. Paul Awoyera
Department of Civil Engineering,
Prince Mohammad Bin Fahd University,
Saudi Arabia.
Email: awopaul2002@gmail.com

Dr. Muhammad Tahir Lakhiar
Shenzhen International Graduate School,
Tsinghua University, China
Email: muhammadtahir@sz.tsinghua.edu.cn

Dr Kalhoro Ghulam Mujtaba
State Key Laboratory of Herbage improvement and Grassland Agro-Ecosystems,
Lanzhou University, China
Email: kalhoro2021@lzu.edu.cn

Dr. Abdul Salam Buller
Department of Civil Engineering,
NED University, Karachi
Email: engr.salam@cloud.neduet.edu.pk

Dr. Muneer Ahmed
Department of Civil Engineering
Roma Tre university, Italy

Email: muneer.ahmed@uniroma3.it

Table of Contents

Aror University Research Journal (ISSN.3106-9797)

https://aurj.aror.edu.pk/aurj

2025, Volume 02, (issue 02) pages 01-05

Design And Simulation of Concrete Beams by Using Fly Ash as a Partial Replacement for Cement

Ghulam Rasool Memon [a,*], Fazul Hussain, Dhanesh Kumar [a]

[a] *Mehran University of Engineering & Technology, Shaheed Zulfiqar Ali Bhutto University, Khairpur Mirs', Sindh, Pakistan*

[*] Corresponding Author: Ghulam Rasool Memon, Email: grmemon05@muetkhp.edu.pk

Received: 20-12-2024, Revision 1: 02-06-2025, Revision 2: 24-12-2025, Accepted: 26-12-2025

KEYWORDS

Fly ash,
Flexural strength,
Crack depth,
ETABS

ABSTRACT

Concrete is one of the most widely used construction materials, but its high demand comes at a significant environmental cost due to the pollution caused by cement production. This research explores a practical and sustainable solution by replacing part of the cement with fly ash and studying its effects on concrete's performance. Among the different mixes tested, concrete with 15% fly ash delivered the best results, achieving a flexural strength of 2.557 MPa—outperforming mixes with 0% and 20% fly ash. It also became easier to work with, as the slump increased from 64 mm to 71 mm with higher fly ash content, improving placement and handling. Crack resistance was also enhanced, with the 15% fly ash mix showing the shallowest crack depth at just 101 mm. This is because fly ash fills tiny gaps in the concrete and reacts with leftover materials, creating a stronger, more durable structure. On the structural side, when this mix was used in building models in ETABS, it showed better resistance to lateral forces, with reduced story displacements in both directions. While there was a slight drop in stiffness, the overall performance of the material improved significantly. These findings highlight how using 15% fly ash in concrete strikes a balance between strength, workability, and sustainability, offering a simple yet impactful way to build greener, more efficient structures.

1. Introduction

Concrete is the heart of modern construction, known for its strength, versatility, and ability to shape the built environment. But behind its widespread use lies a serious challenge: Traditional concrete production relies heavily on cement, which isn't great for the environment because it releases a lot of carbon dioxide when it's made. The manufacturing process of cement releases approximately 0.9 pounds of CO_2 for every pound of cement (Portland Cement Association). This has driven researchers to search for alternatives that reduce the environmental impact of concrete while maintaining its strength and durability. One solution that has gained attention is the use of fly ash (FA), a byproduct of coal combustion in power plants. This is cool because it means we can use less cement, which means less carbon dioxide going into the atmosphere as a by-product of burning coal, fly ash is the residue that is left over after burning coal (Naik et al., 2014). Fly ash is abundant, cost-effective, and has the potential to improve concrete. Studies show that adding fly ash to concrete can enhance its workability, improve durability, and even increase its flexural strength, an essential property for load-bearing elements like beams. What's more, addition of FA as a partial replacement to the concrete may decrease the depth of crack in both mixtures. Applying FA could have the effect of decreasing the depth of fracture spread. (Raj, B. S., & Rao, M. K. 2023). These qualities make it a strong contender for more sustainable construction practices. However, figuring out the best way to use fly ash in concrete beams isn't straightforward. It takes careful testing to find the right balance between reducing cement content and maintaining performance. Advanced tools like ETABS make this task easier by simulating how fly ash concrete beams perform under different loads.

This research dives into how varying levels of fly ash affect the strength, durability, and behavior of concrete beams. By combining real-world testing with ETABS simulations, it aims to reveal how fly ash can be used to its fullest potential. It will also look at how changing the shape of beams can make them even stronger and more sustainable. The goal is to create smarter, greener, and more efficient concrete designs that benefit both the environment and the construction

industry.

2. Material Properties and Methods

2.1 Material Properties

The process of making fly ash beams requires careful planning and execution to meet the desired standards, the necessary materials fly ash, coarse aggregate, fine aggregate, cement, and water are gathered. The first step is too dry mix these materials in proportions to ensure everything is evenly blended. After that, water is added, and the wet mixing begins, creating a smooth, workable mix. This mixture is poured into molds of 150 x 150 x 500 mm, and a 50-second vibration step helps settle and compact the materials properly. After setting it for 24 hours, the beams are carefully removed from the molds and submerged in water for curing, a crucial step that lasts 14 or 28 days to help them gain strength. Once the curing is complete, the beams are taken out, towel-dried, and tested immediately to avoid losing strength. Flexural strength tests are done using a Universal Testing Machine (UTM) with center-point loading, and three specimens from each batch are tested to ensure accurate results. After finding the optimal fly ash content, compressive strength tests are conducted, and the data is used in ETABS to simulate and validate the results. In ETABS, the experimental findings analyze factors like story displacement and stiffness. Combining hands-on testing and advanced simulations ensures that the results are reliable and insightful, paving the way for better use of fly ash in construction.

2.1.1 Fly Ash

Fly ash is a waste material produced after combustion of coal. It is abundantly available in large quantities at the thermal power plants. Class F fly ash is used in this research which is obtained from Rawalpindi. The different percentages of fly ash used are 10%, 15%, and 20%.

2.1.2 Coarse Aggregate:

Coarse Aggregate will be obtained locally from Khairpur. The maximum coarse aggregate size used is 25mm, as prescribed for standard practice C31 according to ASTM C293-02 for flexure strength or modulus of Rupture of concrete using center point loading.

Ordinary Portland cement was used. Cement and fine aggregate or sand were obtained locally from Khairpur.

2.2 Properties of Fly Ash beams

2.2.1 Workability

A conventional metal cone is filled with concrete in three levels, and each layer is compacted using a tamping rod. The concrete's vertical settlement, or slump, is then measured when the cone is removed. The purpose of the test in this study was to ascertain how different fly ash quantities affect the mix's workability.

2.2.2 Flexural Strength or Modulus of Rupture

This property determines the property of withstanding deformation under bending and flexural loads. The flexural strength or modulus of rupture can be determined by following the procedure of ASTM C293-02 by using center point loading.

$$R = \frac{3\,PL}{2bd^2}$$

Where R is MOR, in psi, or MPa, P is the maximum applied load that the testing apparatus indicates, lbf, or N; L is the span length, in, or mm; b is the average width of the specimen, in., or mm; and d is the average depth of the specimen, in, or mm, at the fracture.

2.2.3 Crack Depth Analysis

Crack depth analysis provides insight into the failure mechanisms of beams under applied loads by examining the depth and propagation of cracks. Concrete beams were incrementally loaded until visible cracks formed, and their depths were measured using crack depth gauges or microscopic imaging. The reason behind this test is to evaluate the role of FA in increasing crack resistance and enhancing the durability and stability of the beams.

2.3 Utilizing ETABS

In this study, ETABS was employed to evaluate the structural behavior of beams designed with varying proportions of fly ash, focusing specifically on story displacement and story stiffness. In this study, a 15-storey symmetrical building is taken.

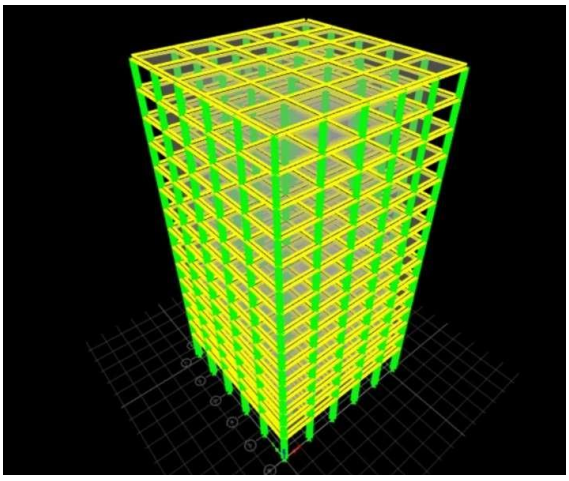

Fig 1: (a) 3D view of building

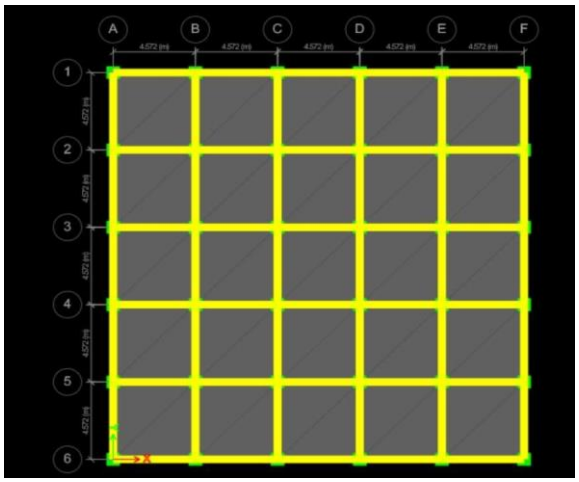

Fig 2: (b) Plan of building

3. Results and Discussion

3.1 Slump Cone Test

Four batches of concrete were prepared with percentages of fly ash being 0%,10%,15%, and 20%. It is found that the usage of fly ash increases the workability of concrete. The role of spherical form of fly ash through its ball bearing influence permits improved mix workability (N Ghazali et al. 2021). The variation in slump pattern shows more workability when a larger amount of fly ash is used, which can be observed in Table 1 and fig 3.

Table 1: Slump Test Results

S NO:	Fly Ash %	Slump (mm)
1	0%	47
2	10%	55
3	15%	64
4	20%	71

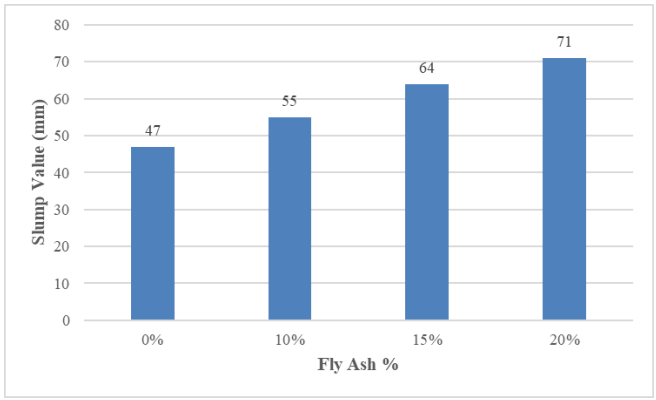

Fig 3: Graph of Slump Test

3.2 Flexural Strength Test

A total of 12 beams are tested for their flexural strength using centre point loading with the help of a universal testing machine. It is observed that flexural strength is found to be maximum at 15% fly ash. The flexural strength or MOR is found by following the procedure of ASTM C293- 02 by using center point loading.

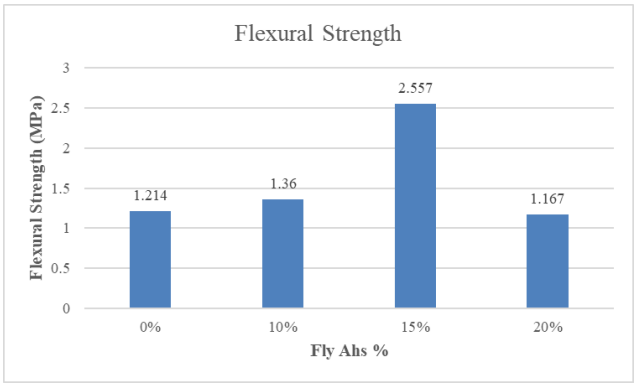

Fig 4: Graph of Flexural Strength Test Results

3.3 Crack Depth Analysis

Crack depths of all 12 beams were observed and measured via tape. The average depth was taken for each batch, and results were obtained. The results of crack depth are minimum at 15% FA and are best understood via graphical representation as shown in Fig 5.

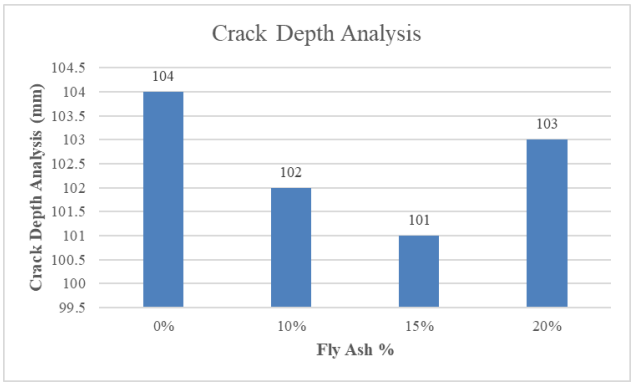

Fig 5: Graph of Crack Depth Analysis

3.4 Results Obtained from ETABS

3.4.1 Story displacement in X-direction

In this study, the performance of concrete with an optimum FA of 15% was compared to that of conventional concrete using ETABS. The findings indicate that the usage of fly ash significantly improves structural behaviour by reducing story displacement in the x-direction. Thus, fly ash concrete demonstrates better performance in resisting lateral loads, making it a more sustainable and effective alternative to conventional concrete in structural applications.

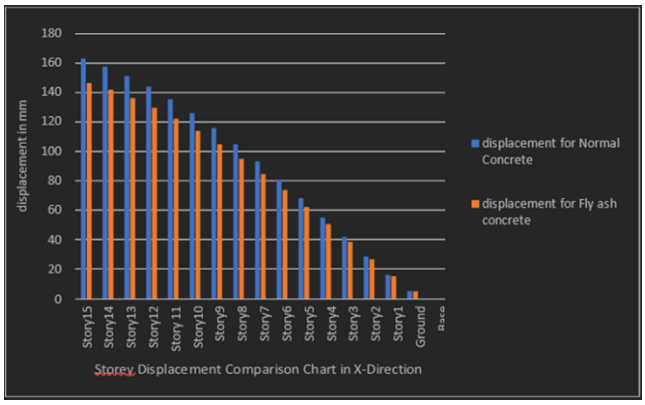

Fig 6: Graph of Comparison Chart of Story Displacement in X-direction

3.4.2 Story displacement in Y-direction

The results of story displacement in the other direction were analysed using ETABS, comparing concrete with 15% FA to conventional concrete. The findings reveal that fly ash concrete exhibits significantly reduced displacement in the y-direction, demonstrating improved stiffness and resistance to lateral loads. These results confirm that incorporating 15% FA not only improves the behavior of concrete under lateral forces but also supports the usage of sustainable materials in construction.

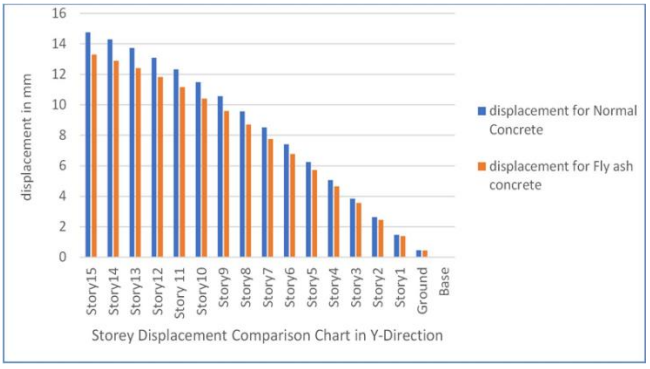

Fig 7: Graph of Comparison Chart of Story Displacement in Y-direction

3.4.3 Story Stiffness in X-direction

The analysis of story stiffness in the x-direction was conducted using ETABS, comparing conventional concrete with concrete containing 15% fly ash. The findings demonstrate that the inclusion of fly ash significantly improves story stiffness, indicating improved resistance to lateral forces.

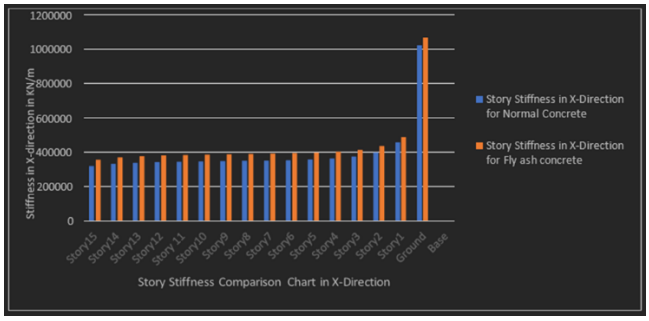

Fig 8: Graph of Comparison Chart of Story Stiffness in X-direction

4. Conclusion

Based on the results from experiments, observations, and ETABS simulations, incorporating 15% fly ash in concrete beams emerges as the ideal choice for balancing strength, workability, and durability. Beams with this mix achieved the highest flexural strength of 2.557 MPa, demonstrated excellent resistance to cracking with a reduced crack depth of 101 mm, and maintained moderate workability with a slump value of 64 mm—striking the perfect balance between ease of placement and stability. Simulations further confirmed the superior performance of 15% fly ash beams, showing reduced lateral displacement and increased stiffness, making them more resilient under load. These findings highlight the potential of 15% fly ash concrete as a sustainable, efficient, and reliable option for modern construction needs.

Acknowledgment

Not available.

Reference

[1] Arivalagan, S. (2009). Flexural Behavior of Reinforced Concrete Beams Containing Fly Ash. International Journal of Structural and Civil Engineering, 1(1).

[2] ASTM International, 100 Barr Harbor Drive, PO Box C700, West Conshohocken, PA 19428-2959, United States. Designation: C 293 – 02

[3] Bielak, J., Schmidt, M., Hegger, J., & Jesse, F. (2020). Structural Behavior of Large- Scale I-Beams with Combined Textile and CFRP Reinforcement. Appl. Sci., 10, 4625. doi:10.3390/app10134625.

[4] Cross, D., Stephens, J., & Vollmer, J. (2005). Structural Applications of 100 Percent Fly Ash Concrete.

[5] Fayed, S., Madenci, E., & Özkılıç, Y. O. (2022). Flexural Behavior of RC Beams with an Abrupt Change in Depth: Experimental Work. Buildings, 12, 2176.

[6] Hawileh, R. A., Mhanna, H. H., & Abdalla, J. A. (2022). Effect of flange geometry on the shear capacity of RC T-beams. Procedia Structural Integrity, 42, 1198–1205. Available online at: [www.sciencedirect.com] (www.sciencedirect.com).

[7] Luca, B. I., Panțiru, A., Timu, A., Bărbuță, M., Diaconu, L. I., Rujanu, M., & Diaconu, A. C. (2023). IOP Conference Series: Materials Science and Engineering, 1283, 012007.

[8] Moolchandani, K.; Sharma,A. Evaluating the Elastic Constants of Concrete, Modified with Fly Ash and Marble Waste, and Their Effects on High-Rise Buildings Using ETABS Software. Sustainability 2023, 15,14743.

[9] Naik, N. S., Jejurkar, C., Naik, N. S., Bahadure, B. M., & Jejurkar, C. L. (2014). Strength and durability of fly ash, cement and gypsum bricks analysis of laminated composites. International Journal of Computational Engineering Research, 04, 2250–3005. [Online] Available at: www.ijceronline.com.

[10] Naik, N. S., Jejurkar, C., Naik, N. S., Bahadure, B. M., & Jejurkar, C. L. (2014). Strength and durability of fly ash, cement and gypsum bricks analysis of laminated composites. International Journal of Computational Engineering Research, 04, 2250– 3005. [Online] Available at: www.ijceronline.com.

[11] Portland Cement Association- the carbon footprint.

[12] Raj, B. S., & Rao, M. K. (2023). IOP Conference Series: Earth and Environmental Science, 1130, 012021.

[13] Siswanto, B., Agus, Salim, M., & Mindiastiwi, T. (2023). The Effect of Fly Ash on the Flexible Strength Concrete and Concrete Temperature. Journal of Survey in Fisheries Sciences, 10(2S), 3133-3141.

[14] Thomas, M. (2007). Optimizing the use of fly ash in concrete. The Portland Cement Organization.

https://aurj.aror.edu.pk/aurj

2025, Volume 02, (issue 02) pages 06-10

"Evaluating the Compressive Strength and Workability Performance of Concrete: Using Demolished Concrete Waste as Fine Aggregate Replacement"

Abdul Qudoos [a,*], Ali Gohar, Dhanesh Vadhvani [a]

[a] *Mehran University of Engineering & Technology, Shaheed Zulfiqar Ali Bhutto University, Khairpur Mir's, Sindh, Pakistan*

[*] Corresponding Author: Abdul Qudoos, Email: *abdulqudooskbr@gmail.com*

Received: 21-12-2024, Revision 1: 02-06-2025, Revision 2: 06-11-2025, Accepted: 26-12-2025

KEYWORDS

Recycled fine aggregates, Sustainable construction, compressive strength, workability,

concrete recycling.

ABSTRACT

Accompanying the increase in awareness of sustainable methods of construction, the need for innovative material efficiency solutions has also arisen. This paper reports a study on the use of RFA manufactured from C&D waste as partial and full replacement of natural fine aggregates in concrete. Concrete with 0%, 50%, and 100% RFA replacement were prepared for investigating their compressive strength and workability. Workability decreased with increased RFA content, with slump values ranging from 14 to 8 to 5 mm for 0%, 50%, and 100% RFA contents, respectively. The control mix achieved a strength of 16.57 MPa at 28 days, while the 50% RFA mix had the highest value of 23.67 MPa-approximately 7 MPa more than that of the control mix. The corresponding strength recorded by the 100% RFA mix was 17.91 MPa, indicating its mediocre performance associated with reduced workability. These results confirm that the replacement level of RFA, which provides the best compromise between strength and workability, is 50%. Hence, it is suitable for non-structural and semi-structural applications. More importantly, the consumption of RFA in concrete manufacturing reduces the demand on natural resource utilization and generates less waste, hence fulfilling some of the key sustainable development criteria within the construction industry.

1. Introduction

After water, concrete is the most consumed material in the world and is considered the backbone of modern infrastructure. The rapid rate of urbanization and increase in population have resulted in an alarming depletion of natural aggregates and exponential rises in construction and demolition wastes. Construction and demolition wastes globally are estimated to comprise 30-40% of total solid wastes, and several countries generate hundreds of millions of tons of wastes annually. In Pakistan, like many developing countries, such wastes are disposed of inefficiently, causing land scarcity, environmental degradation, and unsustainable extractions of natural river sand and other aggregates. Both issues have made the implementation of sustainable construction practices-most notably, the recycling of C&D waste into RFA as a substitute for natural aggregates-imperative. These measures not only help reduce the environmental footprint of the construction industry but also support the development of a circular economy.

Although RFA is expected to be a sustainable alternative, its use in concrete is not exempt from problems. Higher water absorption, induced by the porous nature of RFA, negatively impacts the properties of fresh concretes, especially workability, and can potentially degrade the mechanical performance of hardened concrete. Many investigators have worked on the use of various types of recycled aggregates, but variability in experimental design, curing conditions, and replacement levels has made it difficult to find consistent and comparable trends in the test results. No effort has been systematically made in studying the impact of RFA replacement on both fresh and hardened concrete properties under identical conditions. This calls for further experimentation to establish more clear-cut

evidence of RFA's suitability for conventional concrete mixes.

2. Literature Review

The growing volume of construction and demolition (C&D) waste has made its recycling a crucial element in promoting sustainability within the construction industry. Researchers have shown that incorporating recycled aggregates helps minimize the pressure on landfills and preserves natural resources, all while maintaining acceptable structural performance. For example, Kumar and Kumar (2023) found that the application of recycled aggregates with mineral admixtures can enhance both durability and mechanical strength compared with mixes made from natural aggregates. Similarly, Yehia et al. (2015) identified that even concrete prepared with 100% recycled aggregates can offer acceptable strength and durability, provided the mixture attains a proper packing density.

Using RFA in concrete isn't without its drawbacks. One of the main issues is their higher porosity and greater water absorption, which tend to affect both workability and durability. According to Nanya et al. (2021), using recycle fine aggregate up to about 50% can still meet basic structural requirements. Once the replacement goes beyond that point, the mix becomes noticeably less dense and takes in more water. Berredjem et al. (2020) also pointed out that when natural sand is completely replaced, the concrete shows higher porosity and becomes more vulnerable in harsh environmental conditions. In fact, Jagannadha Rao and Sastri (2016) observed that concrete with recycled aggregates doesn't perform as well as natural aggregate concrete when it comes to acid resistance.

Different methods of pretreatment have received considerable attention in the recent past, mainly to enhance the quality of the RFA. For example, Jean et al. (2024) found that using a carbonation treatment made a clear difference. It increased the density of the material, lowered its water absorption, and even boosted the compressive strength by almost 20% compared to untreated RFA. Cuenca et al. (2021) showed that the recycled ultra-high-performance concrete made using RFA had equivalent durability to the virgin aggregate when supplementary cementitious materials were utilized. Chandar et al. (2018) also suggested that combining the RA with other alternative materials like coconut shells could make durable mixes for non-structural uses.

Various studies confirm the existence of optimum replacement levels. Sai (2018) determined that up to 40% substitution of natural aggregates with recycled aggregates provided acceptable strength and durability, though strength reduction set in at higher levels. Yadav & Pathak (2018) assessed that durability like that of natural aggregates was achieved by processed recycled aggregates with adhered mortar removed. Abadel, in 2023, investigated ultra-high performance geopolymer concrete with recycled fine aggregates and showed that up to 20%, there is no loss of strength, although slight reductions at higher replacement percentages are observed due to weak interfacial bonding.

While significant achievements have been achieved, still certain gaps exist in long-term durability under aggressive conditions. For instance, Gayathri et al. (2025) have demonstrated that the ternary blending of recycled aggregate and fiber can substantially improve resistance against chloride penetration and drying shrinkage, indicating hybrid methods to transcend limitations. Ashwathi et al. (2025) have presented machine learning models for the prediction of recycled aggregate concrete strength, emphasizing AI-driven optimization in mix design.

3. Methodology

3.1 Material and Mix Design

Ordinary Portland Cement conforming to ASTM C150 was used. Crushed stone was used as coarse aggregate, and RFA was obtained from processed waste from construction and demolition activities. The concrete mixes were prepared based on the 1:2:4 proportion. Concrete mixes were prepared based on a 1:2:4 proportion. RFA was added at replacement percentages of 0, 50, and 100%. All mixes had a constant water-cement ratio of 0.6. There is an understanding that the use of a constant water-cement ratio might not result in the optimization of workability or strength performance for each mix, especially at high contents of RFA due to increased water absorption. However, the intention of this study was to provide a consistent baseline for comparison rather than to optimize each mixture individually. The Table 1 below outlines the specific quantities for each component:

Table 1: Mix Composition and Proportions of different batches

Sr.	Replacement %	Cement (kg)	Fine Aggregate (kg)	Replaced Fine Aggregate (kg)	Coarse Aggregate (kg)	Water (kg)
1	0%	8	16	0	32	4.8
2	50%	8	8	8	32	4.8
3	100%	8	0	16	32	4.8

3.2 Experimental Procedures

Material preparation was the first step in the experimental work. Demolition waste concrete was

collected, which was crushed into smaller pieces, and oversized particles were removed by sieving; finally, it was washed to eliminate dust, dirt, and all impurities for proper cleaning to produce clean RFA to be used in mixing. The prepared mixture was mixed using a rotary mixer. In the designed proportions, the cement, natural aggregates, and recycled fine aggregates were added with water and mixed until homogeneous and consistent mass was achieved to ensure the homogeneous distribution of the recycled material in the concrete matrix.

The slump test was conducted immediately after fresh concrete preparation, as outlined in ASTM C143, which stipulates the flowability and ease of handling of concrete. The standard cube specimens of 150 mm were prepared & compacted properly. For each batch, three cubes were prepared and tested in order to obtain reliable average values. These specimens were then submerged in water at room temperature for curing periods of 3 days and 28 days. Subsequently, the cubes were tested for compressive strength on a Universal Testing Machine according to codes ASTM C39. In this way, the effects of RFA replacement on concrete's mechanical properties could be studied systematically.

4. Results and Discussion

4.1 Workability Analysis

The workability of the concrete mixes decreased as the amount of recycled fine aggregate (RFA) increased, as shown by the slump test results in Table 2. The control mix, which contained no RFA, had the highest slump value at 14 mm, indicating better flow and ease of placement. In comparison, the mixes with 50% and 100% RFA showed noticeably lower slump values of 8 mm and 5 mm, respectively. This drop in slump can be mainly linked to the higher water absorption of the recycled aggregates, which reduces the amount of free water available to aid workability.

Based on ASTM C143, slump values in the range of 5–14 mm fall under the “very low” to “low” workability category. Concretes of this type are generally used in applications where high flowability isn’t essential such as mass concrete works, footings, or rigid pavement bases where mechanical vibration assists in proper placement. When better flow and ease of placement are needed, the concrete mix can be fine-tuned—either by using chemical admixtures or tweaking the water–cement ratio. While adding more RFA does make the mix stiffer, it can still be a practical choice for many construction uses where extremely high workability isn’t necessary.

4.2 Compressive Strength of Concrete

The compressive strength results clearly demonstrated that the influence of recycled fine aggregate (RFA) replacement on the performance of the concrete mixes. For 0% RFA, the average compressive strength was 6.69 MPa after 3 days of curing and 16.57 MPa after 28 days, as shown in Table 3. These values stand for the standard mechanical properties of conventional concrete. As shown in Table 4, the compressive strength significantly increased to 9.56 MPa after 3 days and 23.67 MPa after 28 days when 50% of the natural fine aggregates were substituted with RFA. This improvement indicates that partial substitution achieved a well-balanced mix between natural and recycled aggregates, resulting in enhanced internal bonding and more efficient strength development.

Table 2: Workability Analysis

Sr. No	%age of Recycled Fine Aggregate	W/C Ratio	Slump (mm)
1	0%	0.6	14
2	50%	0.6	8
3	100%	0.6	5

The mix including 100% recycled fine aggregate (RFA), on the other hand, achieved average compressive strengths of 6.92 MPa after 3 days and 17.91 MPa after 28 days, as indicated in Table 5. These results are marginally better as compared to the control mix. As illustrated in Figure 1, the fully recycled concrete still trailed behind the 50% replacement mix, particularly in terms of strength gain over time.

Overall, the mix having 50% recycled fine aggregate (RFA) showed noticeably better mechanical behavior in comparison to both standard and fully recycled concretes. It achieved higher compressive strength and performed consistently well, making it suitable for semi-structural elements where only moderate load-bearing capacity is needed. On the other hand, the mix made entirely with RFA, though still usable, tended to be less workable and may face durability issues over time because of its lower slump and greater porosity. Taking these factors together, the 50% replacement level seems to strike the most reasonable balance offering solid strength, manageable workability, and meaningful environmental benefits.

Table 3: Compressive Strength of 0% Replacement

Compressive Strength of 0% Replacement		
Sr. No	**3 Days Compressive Strength (MPa)**	**28 Days Compressive Strength (MPa)**
01	6.15	15.90
02	7.01	16.70
03	6.91	17.12
Average	**6.69**	**16.57**

Table 4: Compressive Strength of 50% Replacement

Compressive Strength of 50% Replacement		
Sr. No	**3 Days Compressive Strength (MPa)**	**28 Days Compressive Strength (MPa)**
01	9.13	22.60
02	10.03	24.84
03	9.51	23.56
Average	**9.56**	**23.67**

Table 5: Compressive Strength of 100% Replacement

Compressive Strength of 100% Replacement		
Sr. No	**3 Days Compressive Strength (MPa)**	**28 Days Compressive Strength (MPa)**
01	7.67	17.76
02	7.27	15.97
03	5.84	20.02
Average	**6.93**	**17.91**

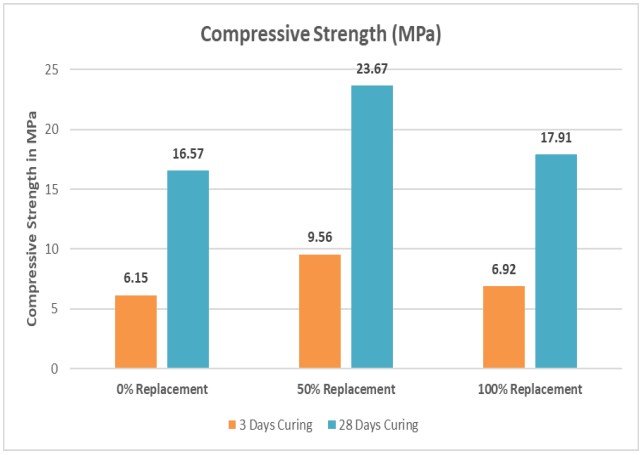

Figure 1: Comparison of 3-day and 28-day compressive strength results for concrete containing 0%, 50%, and 100% Recycled fine aggregate (RFA)

4.3 Practical Implications:

The results of this study indicate that recycled fine aggregates (RFA) can be effectively used in variety of construction work, aligning well with sustainable building techniques. While the control mix showed consistent performance, the mix containing 50% RFA achieved the best overall balance between workability and strength. This makes it a sensible option for semi-structural applications such as elements of low-rise buildings, lightly loaded slabs, or partition walls. On the other hand, the mix with 100% RFA also performed reasonably well but exhibited a noticeable decrease in workability and a slight reduction in strength compared to the 50% mix. Because of this, it seems more suitable for non-structural elements like pedestrian paths, curbstones, and other secondary works. Beyond the technical aspects, using RFA helps reduce the amount of construction and demolition waste sent to landfills and lowers the demand for natural aggregates. Overall, incorporating RFA into concrete manufacturing supports environmental sustainability and can help reduce costs by lowering the need for new raw materials.

5. Conclusion

Results obtained from the study indicate that RFA can serve as a good substitute for natural aggregates in concrete. This is clearly justified from the data obtained. For example, a control mix with 0% RFA attained an average compressive strength of 16.57 MPa at 28 days of age. This is in comparison with the mix with 50% RFA attaining as high a value as 23.67 MPa at the same age-about 7 MPa higher than what was obtained for the conventional mix. Even the 100% RFA mix performed reasonably well, achieving 17.91 MPa, but it was somewhat less effective than the 50% replacement. Overall, the results show that the use of

50% RFA yields the optimum balance of the advantages of strength, workability, and sustainability benefits. This improvement is apparently obtained because of the complementary roles played by natural sand and RFA: while natural sand maintains the density and lowers porosity, RFA adds to surface roughness and helps in internal curing, leading to better packing, bonding, and hydration.

Moreover, the study has few limitations. The water–cement ratio was maintained constant at 0.6 for all mixes, which may not be the optimal value for each replacement level. No chemical admixtures or supplementary cementitious materials were used, either, although these could further enhance workability and strength. Moreover, the curing was done for only 3 and 28 days without any long-term tests for durability. This points out that any future research should look into these shortcomings by focusing on the study of the effects of using admixtures, different curing periods, and durability in various environmental conditions. This would give a complete picture of the uses of RFA in structural and semi-structural applications.

Acknowledgment

Not available

Reference

Abadel, A. (2023). Development of ultra-high performance geopolymer concrete containing recycled fine aggregate replacement. Key Engineering Materials, 970, *33–41.* https://doi.org/10.4028/p-OWola1

Ashwathi, R., Soundariya, R. S., Tharsanee, R. M., Yuvaraj, S., & Ramya, R. (2025). Prediction of strength properties of concrete under the influence of recycled aggregate using machine learning models. Interactions. https://doi.org/10.1007/s10751-024-02189-1

Berredjem, L., Arabi, N., & Molez, L. (2020). Mechanical and durability properties of concrete based on recycled coarse and fine aggregates produced from demolished concrete. Construction and Building Materials, 118421. https://doi.org/10.1016/j.conbuildmat.2020.118421

Chandar, S., Gunasekaran, K., Prasanth, K., & Kumar, G. (2018). An experimental investigation and durability property on recycled concrete with partial replacement to fine aggregate in coconut shell concrete. Research Journal of Chemistry, 11*(2), 702–708.* https://doi.org/10.31788/RJC.2018.1123003

Cuenca, E., Roig-Flores, M., Garofalo, R., Lozano-Násner, M., Ruiz-Muñoz, C., Schillani, F., Borg, R., Ferrara, L., & Serna, P. (2021). Mechanical and durability assessment of concretes obtained from recycled ultra-high performance concretes. RILEM Bookseries. https://doi.org/10.1007/978-3-030-83719-8_81

Gayathri, V., Govardhan, C., Sruthi, S., & Dey, N. (2025). Performance assessment of ternary blended fiber-reinforced recycled aggregate concrete. Research on Engineering Structures and Materials. https://doi.org/10.17515/resm2025-491ma1018rs

Jean, B., Liu, H., Zhu, X., Wang, X., Yan, X., & Ma, T. (2024). Enhancing the mechanical and durability properties of fully recycled aggregate concrete using carbonated recycled fine aggregates. Materials, 17*(8), 1715.* https://doi.org/10.3390/ma17081715

Kumar, K., & Kumar, P. (2023). Comparative study on durability of concrete using recycled and natural aggregate. E3S Web of Conferences, 405, *03018.*https://doi.org/10.1051/e3sconf/202340503018

Nanya, C. S., Ferreira, F. G. da S., & Capuzzo, V. (2021). Mechanical and durability properties of recycled aggregate concrete. Matéria (Rio de Janeiro). https://doi.org/10.1590/s1517-707620210004.1373

Rao, K. J., & Sastri, M. (2016). Durability studies on high strength recycled aggregate concrete. Key Engineering Materials, 708, *70–75.* https://doi.org/10.4028/www.scientific.net/KEM.708.70

Sai, A. (2018). An experimental study on strength properties of concrete using recycled aggregate as replacement in coarse aggregate. International Journal for Research in Applied Science and Engineering Technology, 6*(6), 665–676.* https://doi.org/10.22214/IJRASET.2018.2124

Yadav, S., & Pathak, S. (2018). Durability aspects of recycled aggregate concrete: An experimental study. Journal of Civil and Environmental Engineering, 12, *313–323.* https://doi.org/10.4172/2165-784X.1000313

Yehia, S., Helal, K., Abusharkh, A., Zaher, A., & Istaitiyeh, H. (2015). Strength and durability evaluation of recycled aggregate concrete. International Journal of Concrete Structures and Materials, 9, *219–239.* https://doi.org/10.1007/s40069-015-0100-0

Aror University Research Journal (ISSN.3106-9797)

https://aurj.aror.edu.pk/aurj

2025, Volume 02, (issue 02) pages 11-16

Advanced Structural Analysis and Design G+4 Story Building Using ETABS:

Bisma Latif [a,*], Dhanesh Vadhvani [a], Hassan Nawaz [b]

[a] *Mehran University of Engineering and Technology, Shaheed Zulfiqar Ali Bhutto University, Khairpur Mirs, Sindh, Pakistan*

[b] *National University of Science and Technology, Islamabad, Pakistan*

[*] Corresponding Author: Bisma Latif, Email: bismashaikh056@gmail.com

Received: 22-12-2024, Revision 1: 02-06-2025, Revision 2: 15-12-2025, Accepted: 26-12-2025

KEYWORDS

ETABS,
Multistory Design,
Modal Frequency

ABSTRACT

The growing trend of mid-rise residential and commercial buildings has escalated the demand of precise, reproducible and code-compliant ways of structural analysis. Although ETABS is popular in the field of the design of multi-story buildings, the majority of the current studies are dedicated to software demonstrations, but not to systematic research. A number of prominent researches have demonstrated fundamental abilities of ETABS yet have not explored in-depth research methodologies to be used in conducting rigorous seismic analysis. Nevertheless, this gap has been bridged in our work which explores the seismic and structural performance of G +4 reinforced concrete building in terms of ETABS as per Indian Standards (IS 456:2000, IS 875:1987, IS 1893:2016). The study is valuable in that it offers a thorough research design that will help enhance the use of ETABS in earthquake studies, especially the areas of data validation and improvement of methodology that have not been well addressed in earlier studies. The validation process entailed comparison with the results with known standards and expert verification in order to make them robust and accurate. Nevertheless, the methodology has its weaknesses, such as a possible variation in the properties and conditions of local materials that can affect the generalizability. The methodology will include the determination of the precise grid spacing, the grades of materials (M25 concrete and Fe500 steel) and the loads imposed on it (dead, live, wind, and seismic) and design combinations. The main results are base shear, lateral displacements, bending moments, and reinforcement requirements, which are examined in the framework of code compliance and safety levels. The findings show that the G+4 building satisfies the seismic performance requirements, the basic period is 0.583 seconds, and the frequency is 1.714 Hz, which is ultimately safe and efficient. The results emphasize that ETABS is a powerful tool in cases it is used in the framework of a research-based application as opposed to a tutorial application and the results of the approach are checked against standards and expert validation to confirm their robustness and accuracy.

1. Introduction

As a result of the increasing population, housing and shelter have become essential human needs in high demand. Multi-story structures are being constructed to meet this need. The study and design of these structures can be exceedingly laborious and time-intensive, often requiring weeks or even a month to complete manually. The modern construction requires the use of professional software to facilitate the process. To illustrate, the usage of ETABS software reduces the time of design by approximately 70 percent, which proves that the efficiency is highly improved. This does not just save personnel and time but also provides the right results hence it is easy to implement multiple tasks at once, which can include calculation of shear force, bending moment, reinforcements, deflections and estimation of quantities and costs of the construction. The software has incorporated code books that can assist users design and make structures within the required codes, and this allows the user to work on the designs of

buildings to meet his or her personal interests. Structural analysis can be performed using the various approaches to analysis, and various load combinations can be developed based on the study and design requirements.[1]

The term building is used in Civil Engineering to mean a structure which has been made up of different sections such as foundations, walls, columns, floors, roofs, doors, windows, ventilators, staircases, elevators, and other items that the structure is covered with. The structural analysis and design are used to come up with a structure that is able to withstand all the loads that are put on it without collapsing during its intended lifetime. The analysis and design of any structure should be preceded by the information collection on the supporting soil using a geotechnical investigation that consists in the collection of data and evaluation of the site conditions to guide the foundation construction design and construction. The soil data is an important input of the design models such as the as ETABS, which are an interface of the geotechnical and structural data. This relationship enables a full digital workflow that simplifies the process of transferring ground data collections to models of analysis, thereby enhancing the effectiveness and precision of the design process. The role of the structural engineers will be to achieve the most efficient and cost-effective design, which will ensure that the designed building structure will be functional and viable throughout the intended period. There are currently numerous software tools to analyse and design any sort of structure imaginable.[2]

The most adopted design program in the sector is ETABS. A very large number of design firms use this program in the design of projects. The main goal of the study is the comparative analysis of the data obtained after the manual analysis and the analysis made with the help of ETABS software regarding a multi-storied building structure.[3]

It is not an easy task to build a building that is aesthetically beautiful and rigid enough to withstand severe weather conditions. With technology influencing most of the fields, the aspect of civil engineering needs to be improved tremendously. These have changed the working patterns of the civil engineers. The process has been simplified through the production of specialized software like ETABS-Extended 3D Analysis of Building Systems that has enhanced the quality of the results. ETABS is a holistic program used in construction, planning and designing of buildings which avails a number of options to enable creation of efficient and safe structures. ETABS is competent in solving more complex problems with its in-built modeling tools and code-based load analysis of large building models. It is currently a common tool used in the building of modern structures.[4]

The structural analysis is a measure of the general arrangement and accurate measurements of a particular structure in order to ascertain whether it is serving its purpose and can withstand the forces applied on it throughout its life. The mathematical model of the Burj Khalifa by Skidmore, Owings & Merrill LLP (SOM), was developed using ETABS. The input, output, and numerical solution methods of ETABS are intending to exploit the individual physical and numerical properties of structure of buildings. ETABS is used to test both the static and dynamic loads of a variety of gravity, thermal, and lateral loads. Dynamic analysis can have seismic response spectra or accelerogram time records.[5]

2. Literature Review

K. Naga Sai Gopa and N.Lingeshwaran (2017) [6] designed the structure using ETABS and the LIMIT STATE METHOD for strength, maintainability, durability, and economy. The study focuses on displacement, shear force, and bending moment, emphasizing the need to modify beam and column dimensions and reinforcement if the beam is damaged.

Geethu et.al (2016) [7] compared multilateral building designs with Staad. Pro and ETABS, housing and commercial building projects of the national building code. They discovered that ETABS has always recorded greater values in bending moment and the axial force compared to Staad.pro.

Pawar at.el (2021) [8] modeled a G +4 structure with parking and 2BHK apartments under the codes of IS in view of the static, live, and seismic loads. Considering the analysis, rebar details of the beams as well as columns were acquired.

Varikuppala Krishna at.el 2015 [9] A G + 5 building was analyzed and designed with the ETABS keeping the wind, earthquake, and fire risks in mind. The paper has observed that ETABS is much more cost effective in designing, as it saves about 20 percent per floor in comparison to conventional techniques.

Abhay Guleria (2014) [10] examined some different plan configurations (rectangles, C, L, i-form) of a 15-story RCC building in ETABS. Plans of irregular form enhanced base shear by as much as 15 percent relative

to rectangles, corresponding to the finding that the shape of a plan influences structural performance.

Balaji.U. A, Mr. Selvarasan M.E. B (2016) [11] investigated the seismic loading of a G+13 multi-story residential building through ETABS. Based on the assumption of the linear material characteristics, both a static and dynamic analysis have been conducted, where a nonlinear analysis was done in the high seismic region and in type II soil. Plots of displacement were made and base shear.

Swatantra Kumar Rao and Mr. Kundan Kulbhushan (2019) [12] examined the different types of loads paying attention to shear force and bending moment concerning longitudinal reinforcement. Their findings are useful to the designers to align their analysis with the design codes to facilitate the decision making.

3. Methodology

In order to assess the structural performance of the G+4 building, a systematic approach was used rather than a step wise software tutorial. A major question in the research was put forward. Will a G+4 RC structure studied in ETABS and on the basis of the provisions of IS code pass seismic safety requirements on base shear and displacement The assumptions, modeling strategies and loading conditions used were as follows.

3.1 Model Assumptions:

This type of building is a G+4 reinforced concrete frame type, regular geometry, fixed foundation support and linear type of material behavior.

3.2 Grid and Geometry:

It is made up of 5 bays spaced 4 m in both the X and Y axes and the height of the stories is 3.2 m. Height of the total building is 16 m above the ground.

3.3 Material Properties:

Concrete grade M25 and reinforcement steel Fe500 were assigned. Density of concrete was considered 25 kN/m³.

3.4 Load Definitions:

3.4.1 Dead Load: Self-weight of structural members and wall loads (12 kN/m for external, 8 kN/m for internal walls).

3.4.2 Live Load: 3.0 kN/m² for residential floors as per IS 875 (Part 2).

3.4.3 Wind Load: Applied as per IS 875 (Part 3), with design wind speed 39 m/s.

3.4.4 Seismic Load: Defined as per IS 1893:2016, Zone III, Importance Factor (I) = 1.0, Response Reduction Factor (R) = 5, Soil Type II.

3.5 Load Combinations:

Generated as per IS 456:2000, considering DL, LL, WL, and EQ in both principal directions.

Lateral displacement limits, base shear capacity and the distribution of bending moment were analyzed on the structural model. The results were checked against the allowable code values to provide seismic compliance and safety.

Step:1 Create the Grid

Run the ETABS software. When a model was chosen, a window comes up where one can enter specifications of the grid, such as dimensions and measurements of the building plot. An instance of 2D and 3D structure will then be constructed by the software.

Table 1: Grid lines

Grid System	Grid Direction	Grid ID	Ordinatem
G1	X	A	0
G1	X	B	141
G1	X	C	216
G1	X	D	282
G1	X	E	379.5
G1	X	F	445.5
G1	X	G	520.5
G1	X	H	661.5
G1	Y	1	0
G1	Y	1-	36
G1	Y	2	81
G1	Y	3	222
G1	Y	4	375

Step 2: Define the property

Run the ETABS software. When a model was chosen, a window comes up where one can enter specifications of the grid, such as dimensions and measurements of the building plot. An instance of 2D and 3D structure will then be constructed by the software.

Table 2: Section properties

Name	Mateial
B9x24	Concrete
C12x24	Concrete
Slab5	Concrete

Step 3: Property Assignment

Once the material and section properties have been defined, then use the command menu to build the structural components, define beam lines, and define the columns and regions on which the columns are to be assigned the properties of beam and column sections.

Step 4: Allocating Supports

After the above processes, assign the supports through assignment menu and go to frames and choose fixed.

Step 5: Specify Loads

The loads are defined by choosing the define menu and then, selecting the load cases that are static.

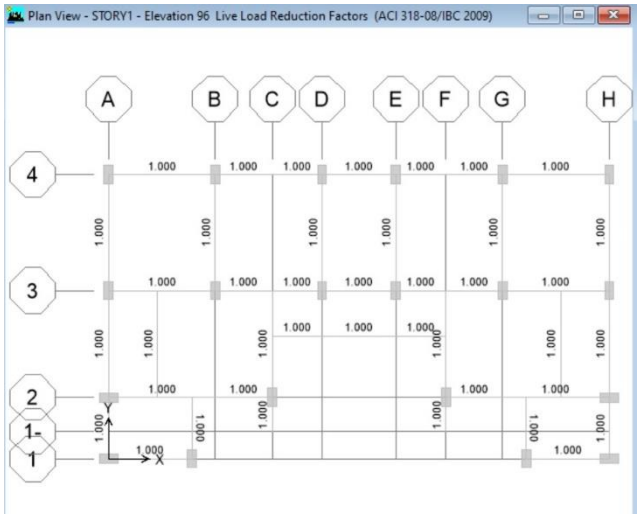

Step 6: Allocation of loads and load combinations

Dead loads are then applied to the exterior and internal walls after determining all the loads. Live loads are applied to the whole building including the finishes on the floor. Wind loads are also calculated and distributed by indicating the direction and wind speed. The determination and assignment of seismic loads are gained by providing input of data on the zone, soil classification, and response modification factor along the X and Y axis. Load combinations are assigned by Load Combinations command in the define menu.

Step 7: Analysis and Design

After the abovementioned processes are completed, analyze the model and check against faults. Begin concrete design process. Choose Design menu, concrete design and select the applicable design options. Then, go back to Design menu and create the concrete frame. ETABS shall assess and plan every structural component as per the selected combinations with the confidence that it would meet design standards.

4. Result and Discussion

A synergistic database helps to merge modeling, analysis and design procedures with the help of the powerful and user-friendly graphical interface of ETABS. CAD drawings can be directly converted into ETABS models. Design of concrete and steel beams, columns, and frames. Construction drawings, encompassing frame plans, details, and cross sections, are generated for concrete and steel structures, while extensive and customizable reports are provided for all analytical and design outputs.

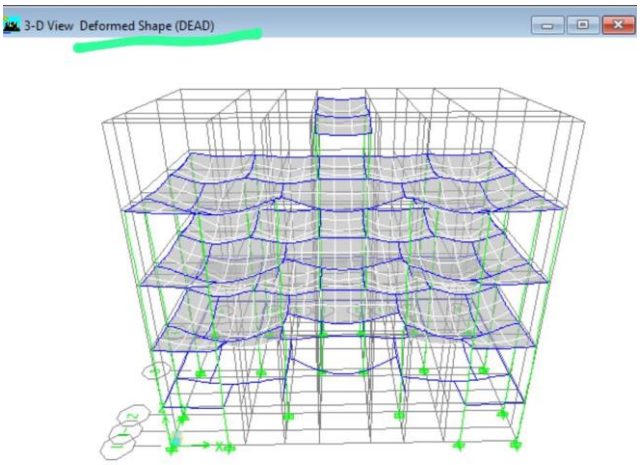

Fig: 3D View After Analysis

Reinforcement:

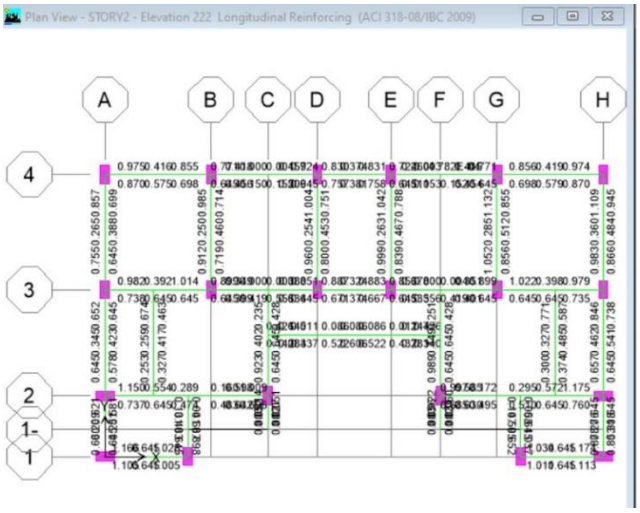

Fig: Longitudinal Reinforcing

Shear Force:

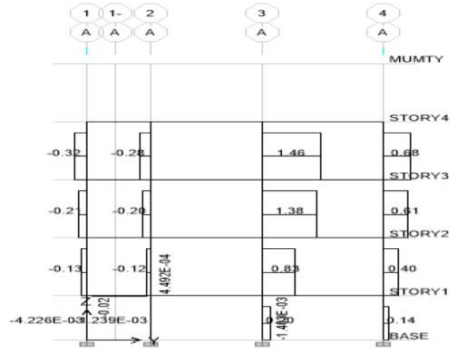

Fig: Base Shear Diagram

Bending Moment:

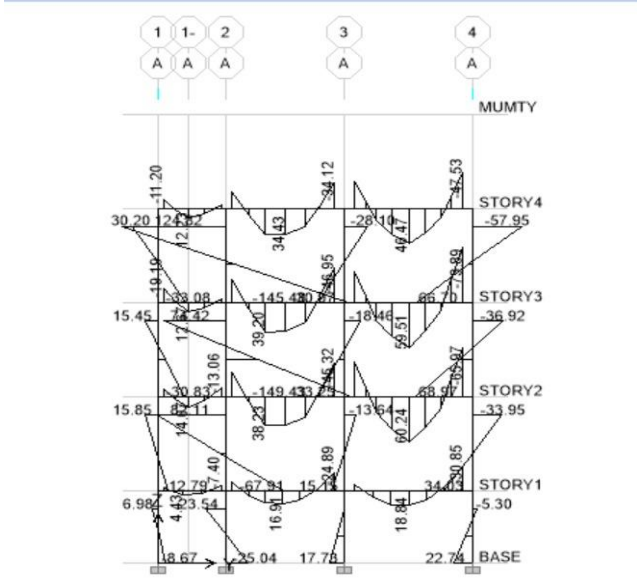

Fig: Bending Moment Diagram

Diaphragms:

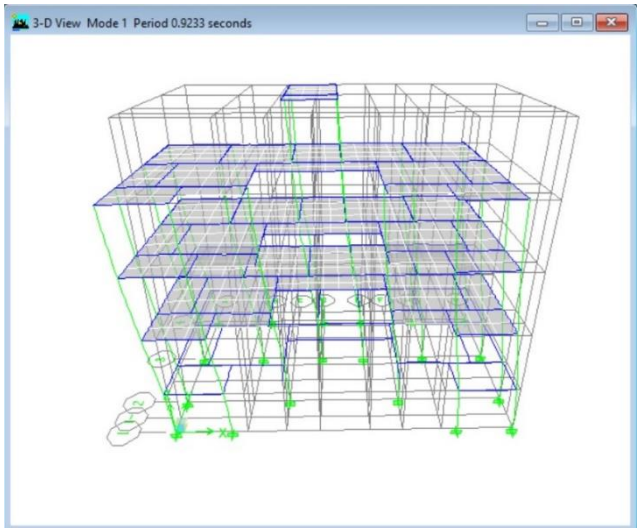

Fig: Diaphragms

Lateral Displacement:

Below is the bar chart of the maximum and average lateral movement of both stories in the X and the Y directions. Contact me on whether you require further modifications or new visualizations.

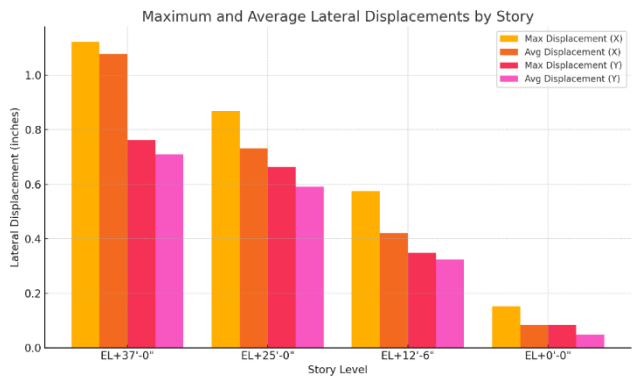

Fig: Lateral Displacement By Story

Seismic Performance:

Mode No	**Duration (seconds)**	**Frequency (Hertz)**	**Circular Frequency (radians per second)**
1	0.58314	1.71485	10.77471

5. Conclusion

The G + 4 RC building is a structure that was studied in terms of structural performance as analyzed through ETABS considering the provisions of the IS code. The experiment revealed that with the right parameters, i.e., grid spacing, material grades, and load definitions in the form of code, the structure fell within the safety limits in both the statical and seismic conditions. The building had a basic period of 0.583 seconds and a frequency of 1.714 Hz, which means that the premises is satisfactorily stiff and stable. The values of base shear and lateral displacement within the allowable IS 1893:2016 limits were acceptable, and, thus, the structure is capable of withstanding the seismic forces safely. This work makes ETABS a research tool of compliance checking against code requirements unlike other works that concentrate on software demonstration. Findings can be used to replicate academic level analysis of mid-rise RC buildings and form a basis of future seismic design studies of such buildings.

The result is detailed shear force and bending moment curves, base shear curves and lateral movement graphs. These will provide critical data concerning the functioning of the building structure. In this case, an example of a top base shear of 1500 kN turns out to be more stable in seismic condition. Besides, the seismic performance indicators such as the natural frequencies and mode shapes testify to the strength of the design. It has a first mode natural frequency of 0.8 Hz.

Accuracy and Efficiency: ETABS makes designing and analysis easier. It saves much time and effort as opposed to manual procedures. It guarantees accuracy of seismic design with the highest inter-story drift ratio of 1%. This transforms the safety and reliability promises into measurable results.

Critical Results: there are the outputs, such as shear force and bending moment diagrams, the base shear analysis and the lateral displacement charts, which supply important information on the structural performance. They also show efficiency and accuracy of the software.

Seismic Reliability: ETABS has seismic reliability in that the software gives engineers certain measures like the natural frequencies, mode shapes, which allow them to confirm the capability of the software to produce safe and reliable designs even in high-dynamic conditions.

Better Visualization: Visualization of design and reinforcing detailing in 3D enhance design accuracy and communicate with stakeholders. As an illustration, in the recent construction of the Skyline Tower, a 45-story residential tower, the development of 3D visualization showed that there was a structural clash. This problem may have postponed the project could it not have been handled at the design stage. Problems were identified early which made it possible to make the necessary changes on time and maintain a smooth flow of communication and cooperation among architects, engineers and contractors.

Viability and Adaptability: ETABS is user friendly and allows customization allowing engineers to solve a broad scope of contemporary engineering problems effectively.

Cost-Effectiveness: ETABS assists in producing cost-effective and robust multi-story buildings, optimizing the design causes, eliminating manual labor, and transferring cost-saving to the projects

Acknowledgment

Not available

Reference

[1] E. U. Syed and K. M. Manzoor, "Analysis and design of buildings using Revit and ETABS software," Mater. Today Proc., vol. 65, pp. 1478–1485, Jan. 2022, doi: 10.1016/j.matpr.2022.04.463.

[2] R. Jose, R. Mathew, S. Devan, and S. Venu, "ANALYSIS AND DESIGN OF COMMERCIAL BUILDING USING ETABS," vol. 04, no. 06.

[3] C. V. S. Lavanya, E. P. Pailey, and M. Sabreen, "Analysis And Design Of G+4 Residential Building Using ETABS".

[4] A. K. Ranja, A. P. Singh, and H. N. Pandey, "Analysis and Design of G+21 Building using ETABS: A Review," Int. J. Res. Appl. Sci. Eng. Technol., vol. 10, no. 3, pp. 1104–1106, Mar. 2022, doi: 10.22214/ijraset.2022.40809.

[5] A. Guleria, "Structural Analysis of a Multi-Storeyed Building using ETABS for different Plan Configurations," Int. J. Eng. Res., vol. 3, no. 5, 2014.

[6] "(PDF) Analysis and design of G+5 residential building by using E-Tabs," ResearchGate, Oct. 2024, Accessed: Dec. 22, 2024. [Online]. Available: https://www.researchgate.net/publication/316967392_Analysis_and_design_of_G5_residential_building_by_using_E-Tabs

[7] I. Journal, "IRJET- Analysis And Design Of Multistorey Building (G+3) By Using ETABS SOFTWARE", Accessed: Dec. 22, 2024. [Online]. Available: https://www.academia.edu/39975146/IRJET_Analysis_And_Design_Of_Multistorey_Building_G_3_By_Using_Etabs_Software

[8] K. Pawar, A. Chavan, A. Ahire, H. Radthod, and J. More, "Analysis, Design and Estimation of G+4 Residential Building," Int. J. Eng. Res., vol. 10, no. 06.

[9] Varikuppala Krishna at.el, "Analysis and Design of Multi Storied Building By Using Etabs Software", Accessed: Dec. 22, 2024. [Online].

[10] A. Guleria, "Structural Analysis of a Multi-Storeyed Building using ETABS for different Plan Configurations," Int. J. Eng. Res., vol. 3, no. 5, 2014.

[11] "Design and Analysis of Multistoreyed Building Under Static and Dynamic Loading Conditions Using Etabs." Accessed: Dec. 22, 2024. [Online]. Available: https://www.ijtra.com/abstract.php?id=design-and-analysis-of-multistoreyed-building-under-static-and-dynamic-loading-conditions-using-etabs-

[12] S. K. Rao and M. K. Kulbhushan, "Design and Analysis of Residential Multistory Building (G+5) by using ETABS," Int. J. Sci. Res. Dev., vol. 7, no. 3, pp. 688–695, Jun. 2019.

Aror University Research Journal (ISSN.3106-9797)

https://aurj.aror.edu.pk/aurj

2025, Volume 02, (issue 02) pages 17-21

Evaluating the Structural Performance of Building Frame and Dual Frame System Incorporating Shear Walls

Ghulam Rasool Memon [a,*], Dhanesh Kumar [a], Zulqarnain Hyder [a], Aizaz Ali [a]

[a] *Mehran University of Engineering & Technology, Shaheed Zulfiqar Ali Bhutto University, Khairpur Mirs', Sindh, Pakistan*

[*] Corresponding Author: Ghulam Rasool Memon, Email: grmemon05@gmail.com

Received: 25-12-2024, Revision 1: 02-06-2025, Revision 2: 05-12-2025, Accepted: 26-12-2025

KEYWORDS

Finite element method, earthquake-resisting buildings, Shear wall, UBC-97, ETABS

ABSTRACT

As cities grow and more high-rise buildings are constructed in earthquake-prone areas, ensuring these structures can withstand seismic forces has become a top priority. In this study, we used ETABS software and the Finite Element Method to analyze and design a G+7 building, focusing on its performance under static and earthquake loads based on UBC-97 standards. We compared two structural systems—a building frame and a dual frame system—to understand how changes in dimensions, material strength, and the placement of shear walls affect the building's safety and stability. The findings showed that positioning the shear wall at the core of the building provides the best results, reducing story drift and displacement while maintaining overall safety. This research emphasizes the importance of smart design choices and modern tools in creating safer, earthquake-resistant buildings that meet the challenges of urban growth.

1. Introduction

The structural design of buildings for seismic loading is primarily concerned with structural safety during major earthquakes. However, serviceability and the potential for economic loss are also concerns [1]. It is crucial to ensure adequate lateral stiffness to resist seismic loads. Other lateral loads such as wind load depend on the building height, wind flow, surrounding exposure, and building shape. It is also significant for multi-story buildings [1]. When the buildings are tall, the dimensions of other structural members also increase and the beam and column sizes become quite heavy, and the steel required is large which makes a lot of congestion at their joints, and it is very difficult to place and vibrate concrete at these places. And because the column of the structure only takes the gravity loads and do not resist the lateral loads so there will be a need for the structural walls, commonly known as shear walls in buildings to resist these seismic forces.

The shapes of the building also affect the result of the shear wall. A shear wall is a structural panel that can resist lateral forces acting on it. Shear walls in symmetrical shapes give better results than asymmetrical shapes as in base shear and story drift [3]. Structural safety is more important; that is why a dual system is adapted to meet the requirement.

The primary objective of this study is to analyze the behavior of a G+7 building frame system and dual frame system incorporating shear walls, and to compare the effects of reducing member dimensions and steel area in both systems with different shear wall placements. Four models were developed by ETABS following the provisions of UBC-97.

The effectiveness of shear walls, structural shapes, and bracing systems in enhancing the seismic performance of high-rise buildings has been extensively explored in recent research. (Barua & Sultana, 2020) analyzed two models, one with a core shear wall and one without and found that the presence of a core shear wall significantly reduced critical parameters like story drift, base shear, overturning moments, column reactions, and maximum bending moments, highlighting the importance of shear walls in improving seismic resistance [1]. Similarly, Chandurkar and Pajgade (2013) explored the impact

of shear wall sizes and concluded that larger shear walls are particularly effective for buildings with more than ten stories, making them both efficient and economical for high-rise construction [2]. In terms of structural shapes, Sultan and Peera (2015) compared rectangular, L-shaped, I-shaped, and C-shaped buildings and discovered that rectangular shapes had the least story drift, while irregular shapes experienced more deformation under seismic forces, emphasizing the advantage of regular, symmetrical designs in minimizing seismic risks [3]. Guleria (2014) further supported these findings, concluding that symmetrical shapes such as rectangular and I-shapes offer superior performance over asymmetrical shapes, as these designs are inherently more stable during earthquakes [9]. In addition, Arlekar et al. (1997) analyzed the importance of ground-story stiffness, suggesting that ground-story columns should be 50% stiffer than upper-story columns to effectively resist seismic forces. Their research also highlighted the critical role of a concrete service core in reducing lateral drift and lowering the strength demand on ground-story columns [4]. Furthermore, the use of bracing systems in steel frames has been shown to significantly increase lateral load resistance. Inamdar and Kumar (2014) demonstrated that ISMB bracing boosts the stiffness of a steel frame by 70%, substantially enhancing its capacity to bear seismic loads [5]. Collectively, these studies underline the importance of shear walls, structural shape, and bracing systems in improving the earthquake resistance of buildings, providing a foundation for further research aimed at optimizing structural safety in high-rise construction.

2. Methodology

This research focuses on examining four different models of a G+7 building to understand how shear walls affect the building's ability to withstand seismic forces. One of the models is designed without shear walls, behaving as a traditional building frame system, while the other three models include shear walls, forming dual systems. The main goal is to analyze the performance of the building frame system, reduce the dimensions of the frame sections to identify potential failure points, and then apply these modified dimensions to the models with shear walls for further analysis.

The four models analyzed in this study are:

1. Building Frame System (no shear walls)
2. Dual System with Four Shear Walls
3. Dual System with Two Shear Walls
4. Dual System with Core Shear Wall

2.1 PLAN and 3D VIEW:

2.1.1 Building Frame System (no shear walls)

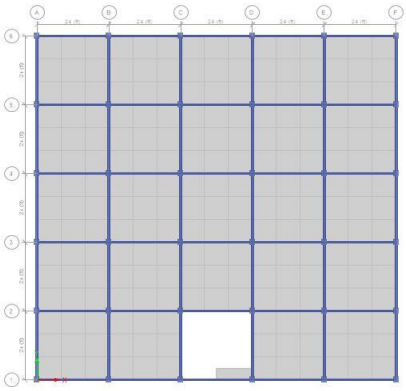

Figure 2.1; *Model 1 Plan view*

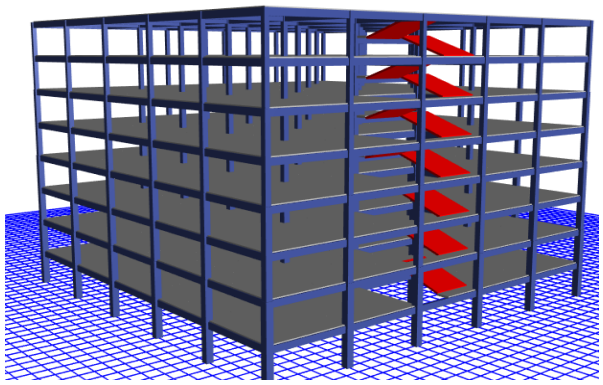

Figure 2.2; *MODEL 1 3D VIEW*

2.1.2 Dual System with Four Shear Walls

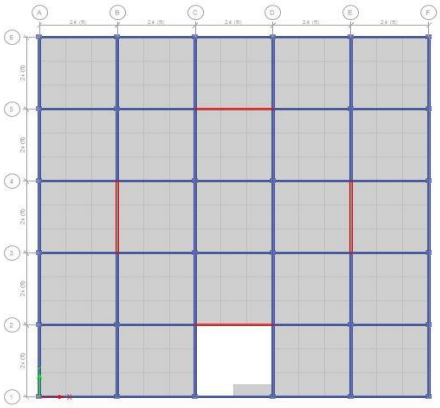

Figure 2.3; *Model 2 Plan view*

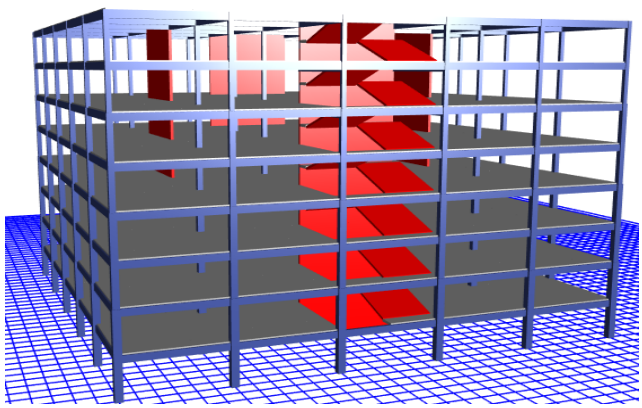

Figure 2.4; *MODEL 2 3D VIEW*

2.1.3 Dual System with Two-Shear Walls

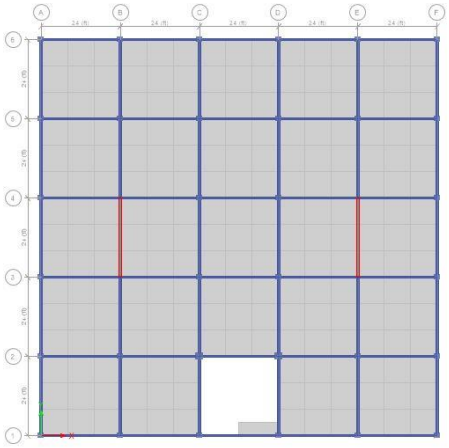

Figure 2.5; *Model 3 Plan view*

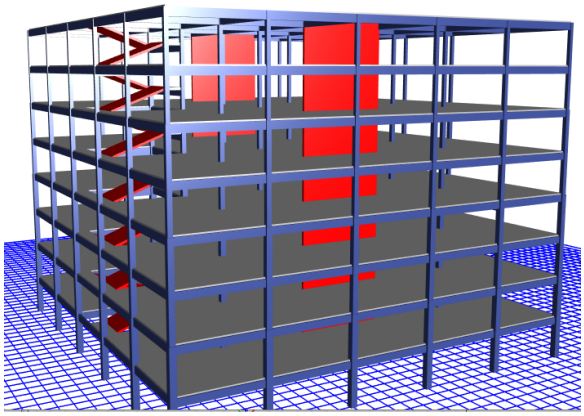

Figure 2.6; *MODEL 3 3D VIEW*

2.1.4 Dual System with Core Shear Wall

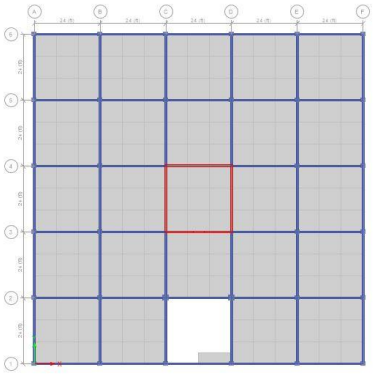

Figure 2.7; *Model 4 Plan view*

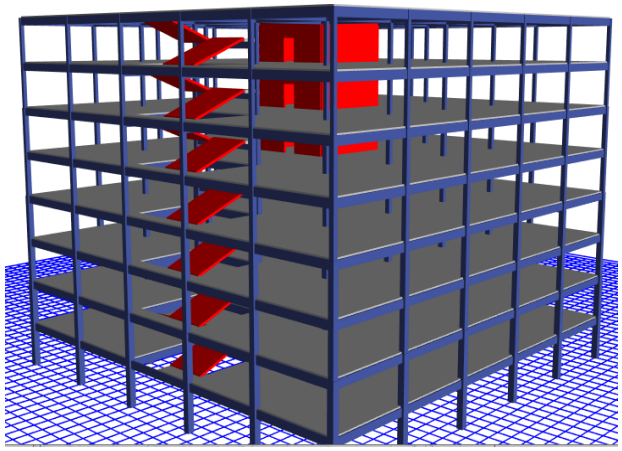

Figure 2.8; *MODEL 4 3D VIEW*

2.2 Material Properties

Material properties for concrete, reinforcement, and steel are summarized in Table 2.1. Frame sections (beams and columns) are listed in Table 2.2, while slabs and wall thicknesses are shown in Table 2.3. Shear walls were modelled as thin shell elements with thicknesses of 9–12 in, depending on their placement.

TABLE: 2.1: Material Properties - Summary

Name	Type	E	v	Unit Weight	Design Strengths
		lb/in²		lb/ft³	
A615Gr60	Rebar	29000000	0.3	490	Fy=60000 lb/in², Fu=90000 lb/in²
C4500	Concrete	3823676	0.2	149.99	Fc=4500 lb/in²
CONC	Concrete	3600000	0.2	149.99	Fc=3000 lb/in²
OTHER	Other	29000000	0.3	489.02	
STEEL	Steel	29000000	0.3	489.02	Fy=50000 lb/in², Fu=65000 lb/in²

TABLE 2.2: Frame Sections - Summary		
Name	**Material**	**Shape**
B8X24	CONC	Concrete Rectangular
B8X27	CONC	Concrete Rectangular
B8X30	CONC	Concrete Rectangular
B8X33	CONC	Concrete Rectangular
C12X12	CONC	Concrete Rectangular
C15X15	CONC	Concrete Rectangular
C15X18	CONC	Concrete Rectangular
C18X18	CONC	Concrete Rectangular
C18X21	CONC	Concrete Rectangular
C21X21	CONC	Concrete Rectangular
C24X27	CONC	Concrete Rectangular

TABLE 2.3: Shell Sections – Summary				
Name	**Design Type**	**Element Type**	**Material**	**Total Thickness**
				in
RW12	Wall	Shell-Thin	4000	12
S5	Slab	Shell-Thin	C3000	5
S6	Slab	Shell-Thin	C3000	6
S7	Slab	Shell-Thin	C3000	7
S8	Slab	Shell-Thin	C3000	8
STAIR8	Slab	Shell-Thin	C3500	8
SW12	Wall	Shell-Thin	C3500	12
SW10	Wall	Shell-Thin	C3500	10
SW9	Wall	Shell-Thin	C3500	9

2.3 Modeling Assumptions

Key assumptions in the modeling included:

a) Rigid diaphragm action was assumed at each floor level.

b) Cracked section stiffness was considered for reinforced concrete members.

c) A damping ratio of 5% was adopted for dynamic response.

4) Shear walls were assumed to be continuous from foundation to roof.

These assumptions reflect standard practice in ETABS modeling for medium-rise reinforced concrete buildings.

2.4 Analysis Procedure

To achieve the research objectives, the methodology followed several key steps. Initially, the models were designed according to the UBC-97 code of practice. Once the design was complete, the models were tested under earthquake loads to assess their seismic performance. The study primarily focused on static analysis, a method that helped determine how the building behaved when subjected to earthquake forces. Key factors like story drift, base shear, and displacement were evaluated to better understand the building's resilience.

By carrying out these analyses, the study aimed to provide valuable insights into how shear wall configurations influenced the structural performance of high-rise buildings during earthquakes, ultimately leading to safer and more efficient designs.

3. Result and Discussion

After the analysis of different positions of shear wall in the building configuration the total members reduced in the models are given below

Model 2 (64 members)

Model 3 (64 members)

Model 4 (64 members)

Also, the comparison in percentage reduction of Story displacement, story drift along with total reduction the area of steel used in the building frame system was carried out. Following tables show the results.

3.1 Story Displacement

After making all members of the models pass, the story displacement is analyzed, and results are calculated as a %reduction in story displacement of Dual models compared to the building frame system. The results are tabulated below:

Table 3.1; *Story Displacement*		
MODEL	**EQX**	**EQY**
MODEL 2	75.88	71.7
MODEL 3	3.37	70.36
MODEL 4	89.01	85.79

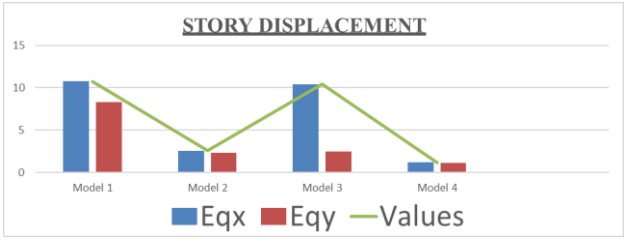

Figure 3.1; Story Displacement Graph

3.2 Story Drift

After making all members of models pass, the story drift is analyzed, and results are calculated as %reduction in story drift of dual models compared to

building frame system. The results are tabulated below:

Table 3.2; Story Drift		
MODEL	**EQX**	**EQY**
MODEL 2	75	72
MODEL 3	11.76	69.89
MODEL 4	89.07	86.02

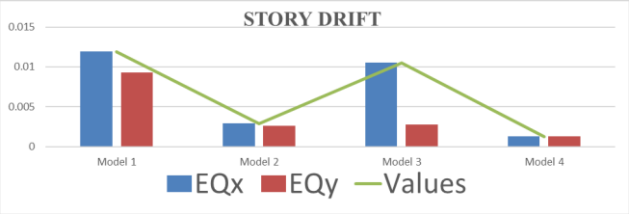

Figure 3.2; Story Drift Graph

3.3 Area of Steel

The area of steel used in column, beam, and shear wall is calculated for all models of building frame and dual frame systems, and the percentage reduction of steel for all dual frame systems is calculated concerning area of steel used in building frame system and is shown in tabulated form.

Table 3.3; Area of Steel Reduction	
MODELS	**% REDUCTION**
MODEL2	34.22
MODEL 3	9.85
MODEL 4	29.76

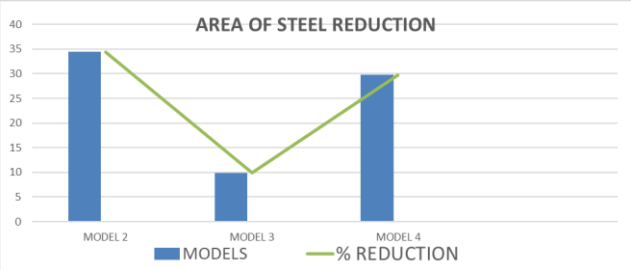

Figure 3.3; Area of steel Reduction

4. Conclusion

Among the models studied, Model 4, which includes a core shear wall, showed clear advantages. Its beam sizes were reduced from 8x24 to 8x12, and 32 columns and beams were removed, making the structure significantly more economical and efficient. The performance of Model 4 stood out in other ways too. It reduced story displacement by 89.01% in the X-direction and 85.07% in the Y-direction, while story drift was reduced by 89.07% in the X-direction and 86.02% in the Y-direction. When it came to material usage, we found that Model 2 achieved the highest reduction in steel area, saving up to 34.22%.

Based on these findings, Model 4 is clearly the best option. It balances safety and cost-effectiveness, reducing story drift and displacement while cutting down on dimensions and materials without compromising strength. This research underscores the importance of incorporating well-designed shear walls in high-rise buildings to improve stability, safety, and efficiency.

Acknowledgment

Not Available

Reference

[1] Barua, S., & Sultana, R. (2020). A Study on Influence of Core Wall in Frame Structure Under Seismic Load.

[2] Chandurkar, P. P., & Pajgade, D. P. (2013). Seismic analysis of RCC building with and without shear wall. International journal of modern engineering research, 3(3), 1805-1810.

[3] Arlekar, J. N., Jain, S. K., & Murty, C. V. R. (1997, November). Seismic response of RC frame buildings with soft first storeys. In Proceedings of the CBRI Golden Jubilee Conference on Natural Hazards in Urban Habitat (pp. 10-11).

[4] Sultan, M. R., & Peera, D. G. (2015). Dynamic analysis of Multi-Storey building for different shapes. International Journal of Innovative Research in Advanced Engineering (IJIRAE), 2.

[5] Inamdar, V., & Kumar, A. (2014). Pushover Analysis of Complex Steel Frame with Bracing Using Etabs.

[6] Panchal, D. R., & Marathe, P. M. (2011). Comparative Study of RCC, steel and composite (G+ 30 storey) building. Nirma University, Ahmedabad, India.

[7] Sirisha, D. (2019). Seismic Analysis and Design of Multistoried Building with and without Bracing According to is Code and Euro Code by using ETABS. International Journal of Engineering Research & Technology, 8(7).

[8] Suryawanshi, A. C., & Bogar, V. M. (2019). Seismic Analysis of Building Resting on Sloping Ground with Soil Structure Interaction. International Research Journal of Engineering and Technology (IRJET) e-ISSN, 2395-0056.

[9] Guleria, A. (2014). structural analysis of a multi-storeyed building using ETABS for different plan configurations. International journal of engineering research and technology, 3(5), 1481-148

https://aurj.aror.edu.pk/aurj

2025, Volume 02, (issue 02) pages 22-28

Production of Ethanol from Apple Peels using Acid Hydrolysis and Fermentation

Abdul Sami Channa [a,*], Danish A. Khokhar [a], Saleem Raza Samo [b], Kishan Chand Mukwana [b]

[a] *Department of Chemical Engineering, Quaid-e-Awam University of Engineering, Science and Technology, Shaheed Benazirabad, Sindh 67450 Pakistan.*

[b] *Environmental Engineering Department, Quaid-e-Awam University of Engineering, Science and Technology, Shaheed Benazirabad, Sindh 67450 Pakistan.*

[*] *Corresponding Author:* Abdul Sami Channa, *E-mail:* abdul.sami@quest.edu.pk

Received: 23-10- 2025, Revision: 23-12-2025, Accepted: 23-12-2025

KEYWORDS

Filtration Application

Energy resource,

ethanol,

apple peels,

acid hydrolysis, fermentation.

ABSTRACT

The increased reliance on food-based feedstock for bioethanol production has intensified concerns related to food security and environmental sustainability. Ethanol is produced from sugar and starchy materials like sugarcane, sugar beet, corn, and wheat. A greater dependence on these crops contributes to the global food crisis. Around 6.96 million tons of fresh fruits are produced in Pakistan, including 0.54 million tons of apples annually. As a result, a massive amount of fruit waste is generated, which is often discarded openly, leading to adverse environmental impacts. This work subjected apple peels to acid hydrolysis and fermentation for ethanol production. The parameters of acid hydrolysis such as particle sizes (149, 210, 297, 590, and 2000 µm), solid loadings (3, 6, 9, 12, and 15 grams (gm)), acid concentrations (4, 8, 12, 16 and 20%), and the hydrolysis time (1, 2, 3, 4 and 5 hours) were investigated. The results showed that the maximum sugar of 15.4˚ Brix was obtained at 9 gm per 50 mL of solid loading with a particle size of 297 µm at a 12% acid concentration in 2 hours of incubation time. The fermentation of apple peel hydrolysate yielded 2.0% (v/v) ethanol. Thus, the results suggested that apple fruit waste can be a potential feedstock for ethanol production. Furthermore, it indicated that bioethanol could be produced from a waste resource, which can help to meet the current energy demands and reduce environmental pollution. This approach not only provides a value-added utilization of agro-industrial waste but also contributes to renewable energy generation, reduced environmental pollution, and decreased dependence on fossil fuels.

1. Introduction

The growing population has diverted the world to industrialization, which increased fossil fuel consumption, depleted the fossil fuel reserves, and adversely impacted the environment [1]. The energy consumption and demands are increasing day by day [2]. The world utilized 88.5 million barrels per day of oil in 2020 [3]. According to expectations, utilization will be 115 million barrels in 2040. The transport sector consumes 57% of liquid fuel, which is the major contributor to COx, SOx, and NOx emissions [4].

The bioethanol production was biomass started from Brazil and the United States in the early 1970s. At present, the ethanol production from biomasses is the best-established process for conversion of biomass to energy. Pakistan is a growing economy globally, where 80% of the population experiences an electricity shortfall of 8 to 10 hours per day in the summer season. According to a study [4], only 60% of the total population has access to electricity. Fossil fuel accounted for 80% of the total energy consumption [4]. Usually, people use biomass as a fuel source for (cooking and heating) in the villages [4]. The government strives to decrease oil consumption and increase reliance on coal or alternate resources. This fossil fuel consumption has also rendered adverse environmental impacts like global warming and

climate change [5]. Pakistan needs an indigenously produced liquid fuel to meet energy requirements in this scenario.

Ethanol is a sustainable, non-toxic liquid fuel that burns cleanly and decreases greenhouse gas emissions. It reduces the environmental damage caused by gasoline combustion. It could be a feasible solution to meet Pakistan's energy, economic and ecological challenges. It can withstand as an alternate transportation liquid fuel, potentially decreasing the dependence on fossil fuels and setting up a supportive back to the economy.

In the past, ethanol was produced only from sugar and starchy materials such as sugarcane, sugar beets, and maize [6]. More dependence on these crops resulted in global food shortages affecting the food supply chain. Furthermore, the price of ethanol feedstocks (corn, sugarcane, sugar beets, potato, wheat, etc.) was also increased [7]. Therefore, these crops cannot meet the worldwide ethanol demand due to their primary value in food and feed [6].

Pakistan is an agricultural country where fruit crops are cultivated up to 7466228 hectares [8]. According to a study, the fruit production is 6.96 million tons, including 0.54 million tons of apples [8]. A large quantity of fruit is utilized in food processing industries to produce jam, jellies, pickles, and fruit juices. Thus, a considerable amount of waste is generated, which is dumped in the landfills or rejected by the environment [3]. Inadequate dumping of such waste could also threaten the groundwater where the water table is high. Also, it is an ecological burden to the environment [9].

This study focuses on bioethanol production from apple peels via acid hydrolysis and fermentation. The acid hydrolysis parameters, such as acid concentration, hydrolysis time, particle size, and solid loading, were investigated for maximum saccharification and ethanol production. Being cost intensive in nature, the treatment of the waste adversely affects the cost of production apple peels and hence it is generally dumped as a waste. So, the production of bioethanol is one of the promising methods to overcome fossil fuels.

2. Materials and Methods

2.1 Collection of Raw Material

The experimental procedure of this work is depicted in Fig. 1. The 4 kg peels of Fuji and Gaja, apple fruit, in mixed form, were collected from a juice shop of the local market at Nawabshah, Pakistan. The physicochemical properties of apple peels are mentioned in Table 1. Laboratory scale concentrated HCl and KOH were purchased from Sigma Aldrich, whereas a 10% KOH solution was prepared in the laboratory. Baker's yeast (Saccharomyces cerevisiae) dried powder was purchased from the chemical shop, and the culture was grown in an Erlenmeyer flask and stored at 4oC [3,10].

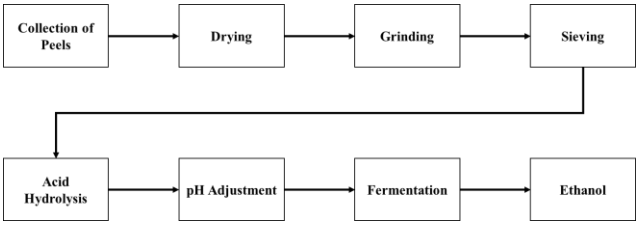

Fig. 1: Process flow chart

2.2 Experimental Procedure

2.2.1 Substrate Preparation

The apple peels were chopped and subjected to grinding in a grinder of model number D-545. Sieve analysis of ground peels was performed to separate in different particle sizes of 2000, 590, 297, 210, and 149 µm of the mesh numbers 10, 30, 50, 70, and 100, respectively, using a sieve shaker Model. No. 881205 (Heiko Seisakusho). Different-sized particles of apple peels were collected and stored for acid hydrolysis.

2.2.2 Acid hydrolysis

Acid hydrolysis of dried ground apple peels was performed at 75oC, with fixed agitation of 120 rpm as suggested by Gebregergs et. al. [11]. Different substrate loadings with five different particle sizes of mesh 10, 30, 50, 70, and 100 were added in 50 mL distilled water at five different acid concentrations to prepare the samples. Each sample was run for 5 hours. Hourly readings were taken to observe the sugar contents. After the hydrolysis, the pH of the solutions was adjusted to 4.9, using a 10% KOH solution. The solution was filtered to remove insoluble particles according to the method reported by Parthiban et. al. [12]. The sugar contents of the solution were checked through the digital Brix meter (model TK-1022).

2.2.3 Yeast Fermentation

The Baker's yeast (Saccharomyces cerevisiae) is a micro-organism that can convert sugar to ethanol and carbon dioxide via the fermentation process [13,14]. Baker's yeast (Saccharomyces cerevisiae) culture was

grown by adding 5 gm of yeast powder in 50 mL distilled water along with 2 mL of H3PO4, 1 mL of H2SO4, and 5 gm of urea in a round bottom flask [15]. Then the solution was kept for agitation at 120 rpm for 36 hours at a temperature of 29oC [1,3]. Later, 10 mL of mature culture was transferred to the maximum saccharified sample for fermentation. The fermentation was carried out at 33oC, 120 rpm, and pH 4.9 [16]. After the fermentation, the ethanol content of the solutions was analyzed using an ebulliometer with its calculating dial [17].

3. Result and Discussion

3.1 Physio-chemical Characteristics of Apple Peels

The composition of apple peels is shown in Table 1, which was taken from the literature [10]. Similar pieces of apple fruit peels were taken for this work. Apple peels contained carbohydrate material that could be solubilized to fermentable sugar. The degree of hydrolysis and its parameters (particle size, acid concentration, solid loading, and hydrolysis time) were investigated in the experimental work.

Parameters	**Range**
Moisture (%)	89.07-90.27
Lipids (%)	0.18-0.35
Proteins (%)	0.30-1.28
Ascorbic acid (%)	0.317-0.322
Fiber (%)	0.87-2.08
Carbohydrates (%)	6.5-9.34
Reducing sugar (%)	0.29-0.97
Total soluble sugar (Brixo)	6.76-6.86
Ash (%)	0.29-0.63
pH	3.53-3.61
All the values are in weight % as per 100 gm of dried sample except soluble sugar and pH.	

Table 1: Physio-chemical characteristics of apple peels [10]

3.2 Acid hydrolysis of apple peels

Table 2 shows the results of sugar yield after 1 hour of hydrolysis. It can be observed that all particle sizes of apple peels were hydrolyzed slowly for lower acid concentrations, while the degradation was faster at the high acid concentrations. For the particle size of 2000 µm, the sugar contents were 1.7˚, 2.1˚, 2.7˚, 3.2˚, and 3.3˚ Brix at acid concentrations of 4, 8, 12, 16, and 20 % (v/v) respectively, with substrate loading of 3 gm. Thus, the sugar contents increased with the increased acid concentration for all the substrate loadings and particle sizes. The maximum sugar of 7.2˚ Brix was achieved at 20% (v/v) acid concentration with 297 µm particle size and 9 gm substrate loading.

The second-hour results of hydrolysis are shown in Table 3. It can be observed that the peels were hydrolyzed rapidly. For the particle size of 2000 µm, sugar yield was increased to 26, 30, 29, 22, and 28% at 4, 8, 12, 16, and 20% (v/v) acid concentrations, respectively, with substrate loading of 3 gm. For the same particle size, at 4% acid concentration, the sugar yield was increased to 26, 34.5, 58.3, 60.8, and 52% for the substrate loadings of 3, 6, 9, 12, and 15 gm, respectively. Results showed that the high solid loading requires more acid to degrade. Whereas, the maximum sugar content of 15.4˚ Brix was achieved after 2 hours at 12% (v/v) acid concentration, 297 µm (mesh 50) particle size, and 9 gm substrate loading.

The third-hour results are shown in Table 4. It can be observed that maximum hydrolyzation occurred within two hours. For the particle size of 2000 µm, an increase in sugar yield was observed with prolonged hydrolysis time. Specifically, at a solid loading of 3 g, the sugar yield increased from 26% to 32%; at 6 g, from 34.5% to 42.4%; at 9 g, from 58.3% to 60%; at 12 g, from 60.8% to 63.3%; and at 15 g, from 52% to 58.6% However, the hydrolysis in the solutions of 3, 6, and 9 gm of mesh 50, 70, and 100 was stopped in the third hour. Sugar yield achieved 15.7º Brix at 9 gm substrate loading for mesh 50 at 12% acid concentration. Thus, the maximum sugar yield was 2% more than achieved in the second hour. In contrast, further increments in acid concentrations lowered the sugar yield. As in the case of particle sizes 590 µm and 297 µm with 6, 9, and 12 gm solid loading, the sugar yield almost decreased with the increase of acid concentration (Table 4).

Hydrolysis almost stopped during the third hour for most of the conditions. However, during the fourth hour, it proceeded to high substrate concentrations of 12 and 15 gm (Table 5). The sugar yield was slightly increased up to 4%. However, the sugar contents were decreased for the lower solid loadings (3, 6, 9 gm) at smaller particle sizes of mesh 50, 70, and 100. Thus, the hydrolysis process almost stopped after the third hour.

The analysis results of the fifth hour hydrolysis time are shown in Table 6. The sugar contents were reduced for all particle sizes, substrate loadings, and acid concentrations. The organic components of peels deteriorated as they were kept in an acidic environment for a long time. This is also in agreement with Cui et. al. [18].

Since multiple factors affect the rate and extent of hydrolyzation, such as particle size, acid

concentration, substrate concentration, and reaction time. Fig. 2(a) shows the effect of substrate concentration and hydrolysis time. The maxi-mum sugar yielded at an acid concentration of 12% and 149 µm particle size. It shows that sugar production increased over time until the first 2 hours. However, a further increase in the hydrolysis time resulted in

Table 2: First-hour hydrolysis results

Particle size	Mesh 10 (2000µm)					Mesh 30 (590µm)					Mesh 50 (297µm)				
Solid loading (gm/50mL)	3	6	9	12	15	3	6	9	12	15	3	6	9	12	15
4% HCl	1.7˚	1.9˚	2˚	1.8˚	1.2˚	2.2˚	3.4˚	4.2˚	3.3˚	2.5˚	2.7˚	3.8˚	4.1˚	3.7˚	3.1˚
8% HCl	2.1˚	2.4˚	2.6˚	2.2˚	1.5˚	3.1˚	4.1˚	5.2˚	4.6˚	3.6˚	3.8˚	5˚	5.9˚	5˚	4.1˚
12% HCl	2.7˚	3.1˚	3.2˚	2.9˚	1.6˚	3.6˚	4.5˚	5.4˚	5.2˚	4.1˚	4˚	5.3˚	6.8˚	5.8˚	4.9˚
16% HCl	3.2˚	3.5˚	3.8˚	3.3˚	1.9˚	3.7˚	4.7˚	5.8˚	5.3˚	4.2˚	4.4˚	5.7˚	6.9˚	5.9˚	5.3˚
20% HCl	3.3˚	3.6˚	4˚	3.2˚	2˚	3.9˚	5.1˚	6.2˚	5.6˚	4.4˚	4.6˚	5.8˚	7.2˚	6.2˚	5.6˚
	Mesh 70 (210µm)					Mesh 100 (149µm)				
Solid loading (gm/50mL)	3	6	9	12	15	3	6	9	12	15
4% HCl	2.5˚	3.1˚	3.9˚	3.4˚	2.9˚	2.3˚	2.7˚	3.6˚	3.2˚	1.8˚
8% HCl	3.4˚	4.3˚	5.3˚	4.5˚	3.6˚	2.9˚	3.9˚	4.9˚	4.2˚	3˚
12% HCl	4˚	4.4˚	6.2˚	5.2˚	4.1˚	3.3˚	4.1˚	5.2˚	4.5˚	3.7˚
16% HCl	4.2˚	4.9˚	6.3˚	5.4˚	4.6˚	3.6˚	4.4˚	5.6˚	4.7˚	4.2˚
20% HCl	4.5˚	5.4˚	6.7˚	5.7˚	4.9˚	3.8˚	4.4˚	5.9˚	5.1˚	4.6˚

Table 3: Second-hour hydrolysis results

Particle size	Mesh 10 (2000µm)					Mesh 30 (590µm)					Mesh 50 (297µm)				
Solid loading (gm/50mL)	3	6	9	12	15	3	6	9	12	15	3	6	9	12	15
4% HCl	2.3˚	2.9˚	4.8˚	4.6˚	2.5˚	3.1˚	3.7˚	5˚	4˚	3.7˚	3.5˚	4.2˚	5.2˚	4.1˚	3.7˚
8% HCl	3˚	3.5˚	6.3˚	5.7˚	3.3˚	3.9˚	4.9˚	7.4˚	6.6˚	5.6˚	4.3˚	6.5˚	7.9˚	6.4˚	5.5˚
12% HCl	3.8˚	4.4˚	8.1˚	7˚	4.5˚	4.6˚	6.5˚	12˚	8.5˚	7.2˚	5.1˚	7.6˚	15.4˚	9.2˚	7.3˚
16% HCl	4.1˚	5.7˚	8.7˚	7.9˚	5.6˚	4.8˚	6.7˚	11˚	9.4˚	7.6˚	4.7˚	7.2˚	12.3˚	10.4˚	8.7˚
20% HCl	4.6˚	6.4˚	9.4˚	8.2˚	6.2˚	4.7˚	6.5˚	10˚	9.8˚	8˚	4.2˚	6.9˚	11.6˚	11˚	9.2˚
	Mesh 70 (210µm)					Mesh 100 (149µm)				
Solid loading (gm/50mL)	3	6	9	12	15	3	6	9	12	15
4% HCl	3.2˚	3.5˚	4.8˚	3.5˚	3˚	2.7˚	3.4˚	4.4˚	4.5˚	2.8˚
8% HCl	3.9˚	5.2˚	7˚	5.5˚	4.8˚	3.4˚	4.1˚	6.7˚	6˚	5˚
12% HCl	4.4˚	6.7˚	13.1˚	8˚	6.5˚	3.9˚	6˚	11.7˚	8.3˚	6.9˚
16% HCl	4.1˚	6.5˚	9.7˚	9.9˚	8˚	3.5˚	4.9˚	10.8˚	9.4˚	8.2˚
20% HCl	3.8˚	5.9˚	9.3˚	10.1˚	8.7˚	3.1˚	4.2˚	10.2˚	9.3˚	9˚

Table 4: Third-hour hydrolysis results

Particle size	Mesh 10 (2000µm)					Mesh 30 (590µm)					Mesh 50 (297µm)				
Solid loading (gm/50mL)	3	6	9	12	15	3	6	9	12	15	3	6	9	12	15
4% HCl	2.5˚	3.3˚	5˚	4.9˚	2.9˚	3.2˚	4.1˚	5.3˚	4.8˚	4.2˚	3.6˚	4.6˚	5.6˚	4.4˚	3.9˚
8% HCl	3.2˚	4.7˚	6.5˚	6.2˚	3.9˚	4.2˚	5.3˚	7.8˚	7.2˚	6.8˚	4.5˚	6.8˚	8.2˚	6.5˚	5.9˚
12% HCl	3.9˚	6˚	9.8˚	8.5˚	5˚	4.9˚	7˚	13˚	9˚	7.6˚	5.2˚	7.9˚	15.7˚	9.7˚	7.9˚
16% HCl	4.3˚	5.9˚	9.1˚	8.7˚	5.8˚	4.7˚	6.9˚	10˚	9.7˚	8.6˚	4.7˚	7.5˚	12.4˚	10.7˚	9.1˚
20% HCl	3.6˚	6.5˚	8.8˚	8.4˚	6.4˚	4.4˚	6.6˚	9.8˚	9.9˚	8.9˚	4˚	7.3˚	10.9˚	10.8˚	9.4˚
	Mesh 70 (210µm)					Mesh 100 (149µm)				
Solid loading (gm/50mL)	3	6	9	12	15	3	6	9	12	15
4% HCl	3.3˚	3.6˚	5.3˚	3.9˚	3.3˚	2.8˚	3.6˚	4.7˚	4.8˚	3.5˚
8% HCl	4.2˚	5.5˚	7.5˚	5.9˚	4.9˚	3.6˚	4.7˚	7˚	6.4˚	5.7˚
12% HCl	4.6˚	6.9˚	13.2˚	8.6˚	7.1˚	4˚	5.9˚	12.1˚	7.8˚	7.7˚
16% HCl	4.5˚	6.9˚	9.9˚	10.1˚	8.6˚	3.7˚	5.9˚	11˚	8.9˚	8.8˚
20% HCl	4˚	6˚	9.6˚	10.2˚	9.1˚	3.4˚	5.7˚	10.4˚	9.8˚	9.5˚

Table 5: Fourth-hour hydrolysis results

Particle size	Mesh 10 (2000µm)					Mesh 30 (590µm)					Mesh 50 (297µm)				
Solid loading (gm/50mL)	3	6	9	12	15	3	6	9	12	15	3	6	9	12	15
4% HCl	2.4˚	3.1˚	4.9˚	5.2˚	3.1˚	3.1˚	4.2˚	5.4˚	4.7˚	3.9˚	3.2˚	4.4˚	5.3˚	4.5˚	4.3˚
8% HCl	2.8˚	4.6˚	6.3˚	6.6˚	4.3˚	4˚	5.5˚	7.6˚	7˚	5.9˚	4.1˚	6.6˚	8˚	6.6˚	6.2˚
12% HCl	3.6˚	5.8˚	9.7˚	9˚	5.2˚	4.7˚	6.8˚	12.5˚	9.7˚	7.7˚	4.6˚	7.5˚	15.2˚	9.9˚	8.5
16% HCl	3.6˚	5.7˚	9.1˚	9.2˚	6˚	4.4˚	6.7˚	10.3˚	9.9˚	7.9˚	4.5˚	7.1˚	12˚	10.8˚	9.3˚
20% HCl	3.5˚	5.4˚	8.7˚	8.7˚	6.5˚	4.3˚	6.1˚	9.4˚	9.2˚	8.2˚	3.5˚	7˚	10.4˚	11˚	9.7˚

	Mesh 70 (210µm)					Mesh 100 (149µm)				
Solid loading (gm/50mL)	3	6	9	12	15	3	6	9	12	15
4% HCl	3.2˚	3.3˚	4.6˚	3.9˚	3.4˚	2.4˚	3.2˚	4.1˚	4.9˚	3.6˚
8% HCl	4˚	5.1˚	7.1˚	6˚	4.9˚	3.3˚	4.4˚	6.6˚	7˚	5.9˚
12% HCl	4.1˚	6.4˚	12.8˚	8.8˚	7.3˚	3.6˚	5.5˚	10.8˚	10.3˚	8˚
16% HCl	4˚	6.5˚	9.3˚	10.7˚	8.9˚	3.3˚	5.2˚	10.1˚	9.6˚	9.5˚
20% HCl	3.3˚	5.4˚	9.2˚	10.5˚	9.5˚	3.1˚	5˚	9.1˚	8.5˚	9.6˚

Table 6: Fifth-hour hydrolysis results

Particle size	**Mesh 10 (2000µm)**					**Mesh 30 (590µm)**					**Mesh 50 (297µm)**				
Solid loading (gm/50mL)	3	6	9	12	15	3	6	9	12	15	3	6	9	12	15
4% HCl	1.8˚	2.0˚	3.8˚	3.3˚	1.3˚	1.4˚	2.7˚	3.6˚	2.3˚	2.7˚	2.1˚	2.7˚	3.0˚	3.1˚	2.1˚
8% HCl	1.9˚	3.3˚	4.4˚	4.6˚	1.9˚	2.4˚	3.6˚	5.1˚	4.6˚	4.1˚	2.6˚	3.9˚	5.3˚	4.7˚	3.8˚
12% HCl	2.7˚	3.8˚	7.3˚	6.7˚	2.1˚	2.8˚	4.9˚	10˚	6.8˚	5.4˚	3.2˚	4.2˚	11.5˚	8.2˚	5.6˚
16% HCl	2.3˚	3.9˚	6.8˚	6.1˚	3.4˚	2.7˚	4.7˚	7.1˚	7.3˚	4.8˚	2.7˚	5.1˚	9.3˚	9.1˚	6.9˚
20% HCl	2.4˚	3.4˚	6.1˚	6.5˚	2.6˚	2.0˚	4.0˚	6.5˚	6.8˚	5.1˚	1.5˚	4.9˚	7.7˚	9.2˚	7.6˚
	Mesh 70 (210µm)					**Mesh 100 (149µm)**				
Solid loading (gm/50mL)	3	6	9	12	15	3	6	9	12	15
4% HCl	1.4˚	1.9˚	2.8˚	2.7˚	1.8˚	1.1˚	2.1˚	2.4˚	3.6˚	2.0˚
8% HCl	1.9˚	3.0˚	4.7˚	3.9˚	2.6˚	1.5˚	1.3˚	3.2˚	4.5˚	3.6˚
12% HCl	1.9˚	3.7˚	8.9˚	5.9˚	5.2˚	1.9˚	2.9˚	6.9˚	7.9˚	5.7˚
16% HCl	2.3˚	3.2˚	6.2˚	7.9˚	6.3˚	1.4˚	2.7˚	5.8˚	7.1˚	6.8˚
20% HCl	1.6˚	2.9˚	5.8˚	8.6˚	6.7˚	1.4˚	2.6˚	5.2˚	7.5˚	6.4˚

reduced sugar contents. This could be attributed due to the catalytic activity of HCl at an optimum concentration which improved the rate of hydrolysis. In contrast, no significant increase in sugar yield was observed beyond 2 hours.

Since multiple factors affect the rate and extent of hydrolyzation, such as particle size, acid concentration, substrate concentration, and reaction time. Fig. 2(a) shows the effect of substrate concentration and hydrolysis time. The maximum sugar yielded at an acid concentration of 12% and 149 µm particle size. It shows that sugar production increased over time until the first 2 hours. However, a further increase in the hydrolysis time resulted in reduced sugar contents. This could be attributed due to the catalytic activity of HCl at an optimum concentration which improved the rate of hydrolysis. In contrast, no significant increase in sugar yield was observed beyond 2 hours.

As shown in Fig. 2(b), particle size also affected the sugar contents. The maximum hydrolyzation was achieved at 297 µm while larger particles declined the sugar yield. At 2000 µm particle size, sugar yield was 3.8˚, 4.7 ˚, 5.1 ˚, 4.5 ˚, and 3.9˚ against the substrate loading 3, 6, 9, 12, and 15 gm, respectively. Maximum production was achieved at 9 gm loading, where the sugar yield was observed at 5.1˚, 7.1˚, 15.5˚, 15.8˚, and 15.3˚ against the particle size 2000, 590, 297, 210, and 149 µm respectively.

Acid concentration also has affected sugar yield during hydrolysis (Fig. 2 (c)). At the optimum solid loading and particle size of the substrate, the maximum sugar yield was achieved at a 12% acid concentration. Therefore, the optimum acid concentration was 12% against 9 gm solid loading with 297 µm particle size.

Thus, 9 gm substrate concentration of 297µm particle size at 12% acid concentration for 2 hours hydrolysis time yielded maximum sugar of 15.4o Brix. The sample above was then subjected to the fermentation process.

3.3 Fermentation of the Hydrolysate

The hydrolysate mixture of apple peels with the highest sugar was neutralized before being subjected to fer-mentation. Then grown yeast culture was transferred to a hydrolysate mixture. The fermentation was performed for 36 hours in the round bottom flask at 33˚C and 120 rpm. The fermentation process yielded 2% v/v ethanol in the hydrolysate mixture separated by distillation. Different researchers used various fruit peels for ethanol production. Oberoi et. al. [19] used orange peels and produced 0.46 gm/gm ethanol per substrate consumed. Abidin et. al. [20] used cassava peel (Manihot esculenta) and obtained 3.58 % v/v bioethanol. Mushimiyimana and Tallapragada [21] used carrot, onion, potato, and sugar beet peel and achieved ethanol production of 2.2, 14.4, 15.3, and 17.3%, respectively. In addition, Saleem et. al. [22] used Pomegranate waste peels and achieved 0.42 ± 0.08 gm/gm ethanol per substrate consumed. In this study, apple peels yielded 15.7˚ of sugar via acid hydrolysis and 2% v/v ethanol during the fermentation process.

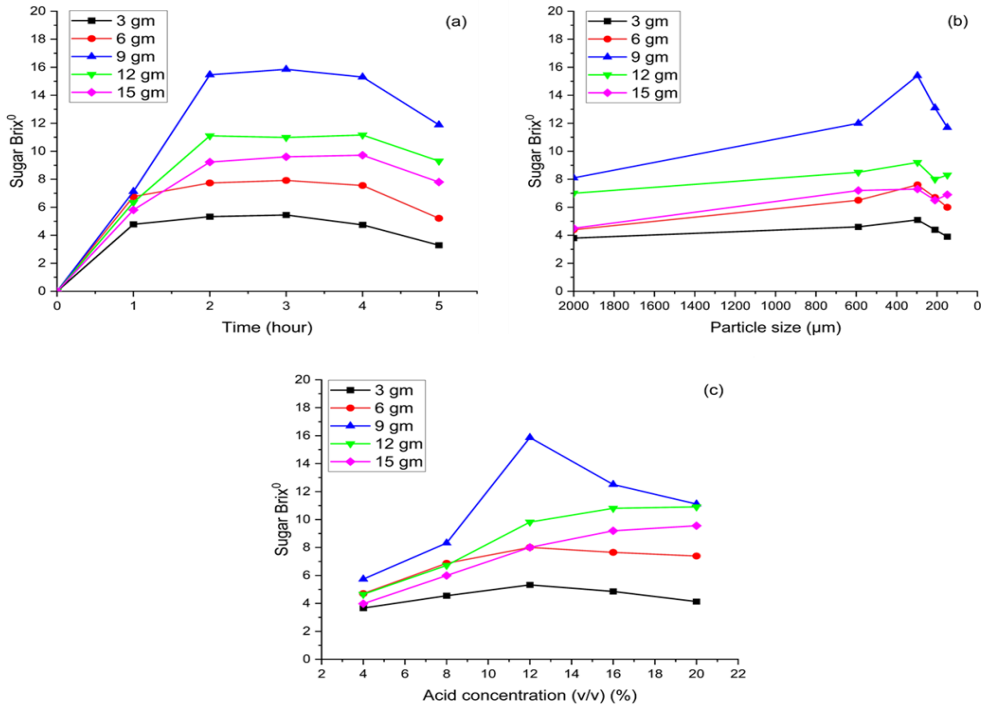

Fig. 2: Effect of (a) hydrolysis time, (b) particle size, and (c) acid concentration on sugar yield during acid hydrolysis of apple peels at different solid loadings.

4. Conclusion

The effect of different parameters such as particle sizes (149, 210, 297, 590, and 2000 µm), solid loadings (3, 6, 9, 12, and 15 gm/50 mL), acid concentrations (4, 8, 12, 16 and 20%), and the incubation time (1,2 3, 4 and 5 hours) was investigated during the acid hydrolysis of apple peels. The apple peel hydrolysate was also subjected to fermentation for bioethanol production. The results showed that the maximum sugar content of 15.4˚ Brix has achieved at 9 gm solid loading per 50 mL, with a particle size of 297 µm at 12% acid concentration in a 2-hour incubation time. The fermentation of apple peels hydrolysate yielded 2.0% v/v ethanol. The study's findings suggest that lower solid loadings can yield high sugar contents with a high rate of hydrolysis. Furthermore, the larger particle size of peels produced less sugar with a long hydrolysis time. In addition, the exposure of peels to the acid for an extended time at high temperatures can deteriorate peels' organic contents, resulting in less sugar content. The study suggests fruit peels from the food industry as the potential feedstock for ethanol production. Furthermore, it provides an insight into bioethanol production from waste resources. This can help meet the current energy demands with less economic burden and minimize environmental pollution.

Acknowledgment

Not available

Reference

[1] Ye Sun and Jiayang Cheng, "Hydrolysis of lignocellulosic materials for ethanol production: a review," Bioresource technology.Vol. 83, No.1, pp. 1-11, 2002.

[2] Abdur Raheem, Mohammad Yusri Hassan and Rabia Shakoor, "Bioenergy from anaerobic digestion in Pakistan: Potential, development and prospects," Renewable and Sustainable Energy Reviews.Vol. 59, pp. 264-275, 2016.

[3] In Seong Choi, Yoon Gyo Lee, Sarmir Kumar Khanal, Bok Jae Park and Hyeun-Jong Bae, "A low-energy, cost-effective approach to fruit and citrus peel waste processing for bioethanol production," Applied Energy.Vol. 140, pp. 65-74, 2015.

[4] Hans-Wilhelm Schiffer, Tom Kober and Evangelos %J Zeitschrift für Energiewirtschaft Panos, "World energy council's global energy scenarios to 2060."Vol. 42, No.2, pp. 91-102, 2018.

[5] Muhammad Imran Qureshi, Usama Awan, Zeeshan Arshad, Amran Md. Rasli, Khalid Zaman and Faisal Khan, "Dynamic linkages among energy consumption, air pollution, greenhouse gas emissions and agricultural production in Pakistan: sustainable agriculture key to policy success," Natural Hazards.Vol. 84, No.1, pp. 367-381, 2016.

[6] Anubhuti Gupta and Jay Prakash Verma, "Sustainable bio-ethanol production from agro-residues: A review," Renewable and Sustainable Energy Reviews.Vol. 41, pp. 550-567, 2015.

[7] Farid Talebnia, Dimitar Karakashev and Irini Angelidaki, "Production of bioethanol from wheat straw: An overview on pretreatment, hydrolysis and fermentation," Bioresource Technology.Vol. 101, No.13, pp. 4744-4753, 2010.

[8] Economic Wing, "Fruit Vegetables and Condiments Statistics of Pakistan 2018-19," Ministry of National Food Security & Research, 2020. Available from: http://www.mnfsr.gov.pk/frmDetails.aspx

[9] Amit Bhatnagar, Mika Sillanpää and Anna Witek-Krowiak, "Agricultural waste peels as versatile biomass for water purification – A review," Chemical Engineering Journal.Vol. 270, pp. 244-271, 2015.

[10] Polyana Campos Nunes, Jailane de Souza Aquino, Ismael Ivan Rockenbach and Tânia Lúcia Montenegro Stamford, "Physico-Chemical Characterization, Bioactive Compounds and Antioxidant Activity of Malay Apple [<italic>Syzygium malaccense</italic> (L.) Merr. & L.M. Perry]," PLoS ONE.Vol. 11, No.6, pp. e0158134, 2016.

[11] Alula Gebregergs, Mebrahtom Gebresemati and Omprakash Sahu, "Industrial ethanol from banana peels for developing countries: Response surface methodology," Pacific Science Review A: Natural Science and Engineering, 2016.

[12] R. Parthiban, M. Sivarajan and M. Sukumar. "Ethanol production from banana peel waste using Saccharomyces cerevisiae," in Sustainable Energy and Intelligent Systems (SEISCON 2011), International Conference on. of Conference. pp. 177-183.Year.

[13] Monisha Abbi, Ramesh Chander Kuhad and Ajay Singh, "Bioconversion of pentose sugars to ethanol by free and immobilized cells of Candida shehatae (NCL-3501): Fermentation behaviour," Process Biochemistry.Vol. 31, No.6, pp. 555-560, 1996.

[14] Ja Kyong Ko, Youngsoon Um, Han Min Woo, Kyoung Heon Kim and Sun-Mi Lee, "Ethanol production from lignocellulosic hydrolysates using engineered Saccharomyces cerevisiae harboring xylose isomerase-based pathway," Bioresource Technology.Vol. 209, pp. 290-296, 2016.

[15] M Ballesteros, JM Oliva, P Manzanares, M Jand Negro and I Ballesteros, "Ethanol production from paper material using a simultaneous saccharification and fermentation system in a fed-batch basis," World Journal of Microbiology and Biotechnology.Vol. 18, No.6, pp. 559-561, 2002.

[16] Mark R. Wilkins, Wilbur W. Widmer and Karel Grohmann, "Simultaneous saccharification and fermentation of citrus peel waste by Saccharomyces cerevisiae to produce ethanol," Process Biochemistry.Vol. 42, No.12, pp. 1614-1619, 2007.

[17] Phitchaphorn Khammee, Yuwalee Unpaprom, Chudapak Chaichompoo, Piyapit Khonkaen and Rameshprabu %J 3 Biotech Ramaraj, "Appropriateness of waste jasmine flower for bioethanol conversion with enzymatic hydrolysis: Sustainable development on green fuel production."Vol. 11, No.5, pp. 1-13, 2021.

[18] Jingang Cui, Dawei Qi and Xue %J Ultrasonics Sonochemistry Wang, "Research on the techniques of ultrasound-assisted liquid-phase peeling, thermal oxidation peeling and acid-base chemical peeling for ultra-thin graphite carbon nitride nanosheets."Vol. 48, pp. 181-187, 2018.

[19] Harinder Singh Oberoi, Praveen Venkata Vadlani, Ronald L Madl, Lavudi Saida, Jithma P %J Journal of agricultural Abeykoon and food chemistry, "Ethanol production from orange peels: two-stage hydrolysis and fermentation studies using optimized parameters through experimental design."Vol. 58, No.6, pp. 3422-3429, 2010.

[20] Zainal Abidin, Ellena Saraswati and Tadjuddin %J Int J PharmTech Res Naid, "Bioethanol production from waste of the cassava peel (Manihot esculenta) by acid hydrolysis and fermentation process."Vol. 6, pp. 1209-1212, 2014.

[21] Isaie Mushimiyimana and Padmavathi Tallapragada, "Bioethanol production from agro wastes by acid hydrolysis and fermentation process," 2016.

[22] Ayesha Saleem, Ali Hussain, Asma Chaudhary, Qurat-ul-Ain Ahmad, Mehwish Iqtedar, Arshad Javid, Afia Muhammad %J Biomass Conversion Akram and Biorefinery, "Acid hydrolysis optimization of pomegranate peels waste using response surface methodology for ethanol production," pp. 1-12, 2020.